Polarimetry of Extrasolar Planets

Phil Lucas

University of Hertfordshire,

England

Polarised Light

- In general light waves are elliptically polarised. However it is always possible to express a light wave as the sum of an unpolarised wave, a 100% linearly polarised wave and a 100% circularly polarised wave.

- $I_{tot} = I_{Upol} + I_{Lpol} + I_{Cpol}$

Polarised Light

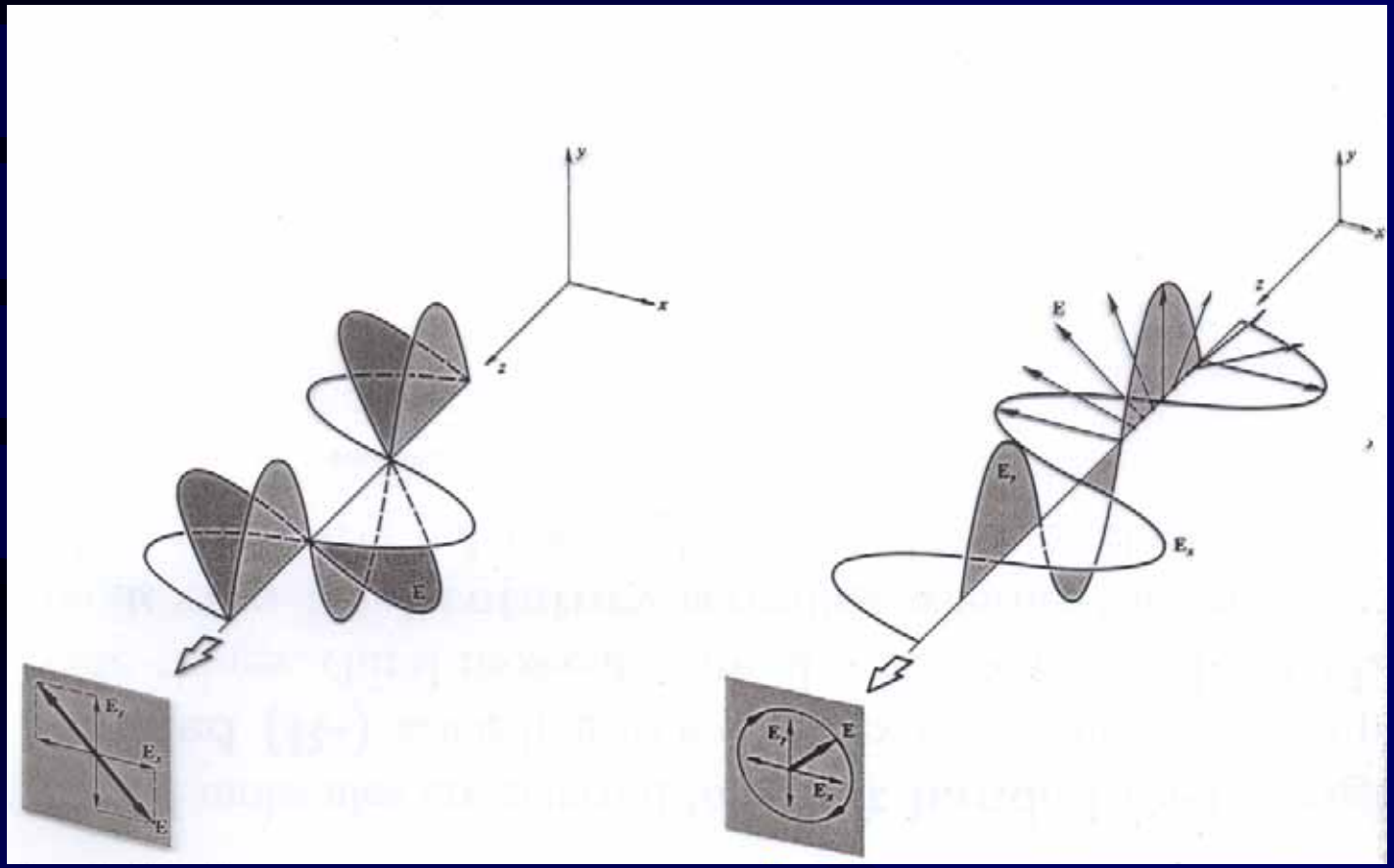

Linear Pol

Circular Pol

Stokes Vectors

- The polarisation state is most commonly represented by a Stokes vector. Stokes vectors from different light rays can be added linearly, which makes them easy to use.
- S = (I,Q,U,V)
- I=Total flux
- $Q=(I_0 - I_{90})/(I_0 + I_{90})$
- $U=(I_{45} - I_{135})/(I_{45} + I_{135})$
- V=Cpol flux (right handed Cpol or left handed Cpol taken as positive by different people).
- $P=SQRT(Q^2 + U^2 + V^2)/I$

Polarimetry of Solar System Planets

- **Strong limitation on phase angles for the planets of the outer solar system means that most useful data are from space.**
- **Pioneer 10 and Pioneer 11. Observed Jupiter and Saturn in 1973,1974. Eg. Smith & Tomasko 1984, Icarus 58, 35**
- **Galileo – further polarimetry of Jupiter in 1996 (Braak et al.2002, Icarus 157, 401).**
- **High polarisation seen in places, attributed to sub-micron haze particles and Rayleigh scattering. Low polarisation attributed to a deeper cloud layer of different sub-micron particles.**
- **Polarisation varies between dark belts and bright zones and is far higher at high latitudes than at the equator.**

Polarimetry of Solar System Planets

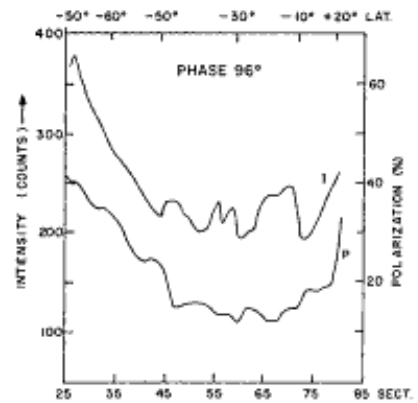

Fig. 6. Intensity and polarization of blue light as a function of sector (representing one field of view) and latitude along a scan in a roughly north-south direction for the southern hemisphere. The data were received 2 hours, 16 minutes before pericenter at a phase angle of ~ 96°.

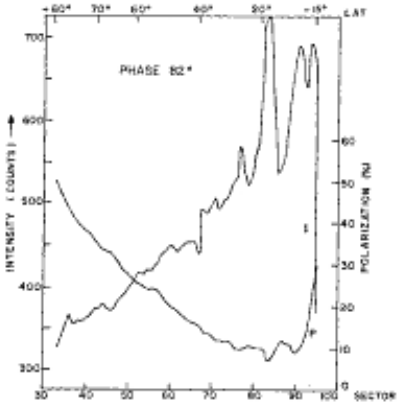

Fig. 7. Intensity and polarization of blue light as a function of sector (representing one field of view) and latitude along a scan in a roughly north-south direction for the northern hemisphere. The data were received 2 hours, 4 minutes after pericenter at a phase angle of ~ 82°.

Polarimetry of Solar System Planets

Venus. – polarimetry was used to discover that the main cloud layer is composed of 1um sized sulphuric acid droplets rather than water. This was done by fitting the refractive index with a precision of +/- 0.01.

Mars – Circular polarimetry is being used to search for organic molecules in the crust. Solid matt surfaces generally give a low polarisation.

Earth – smooth liquid surfaces found in the oceans produce high polarisation by specular reflection.

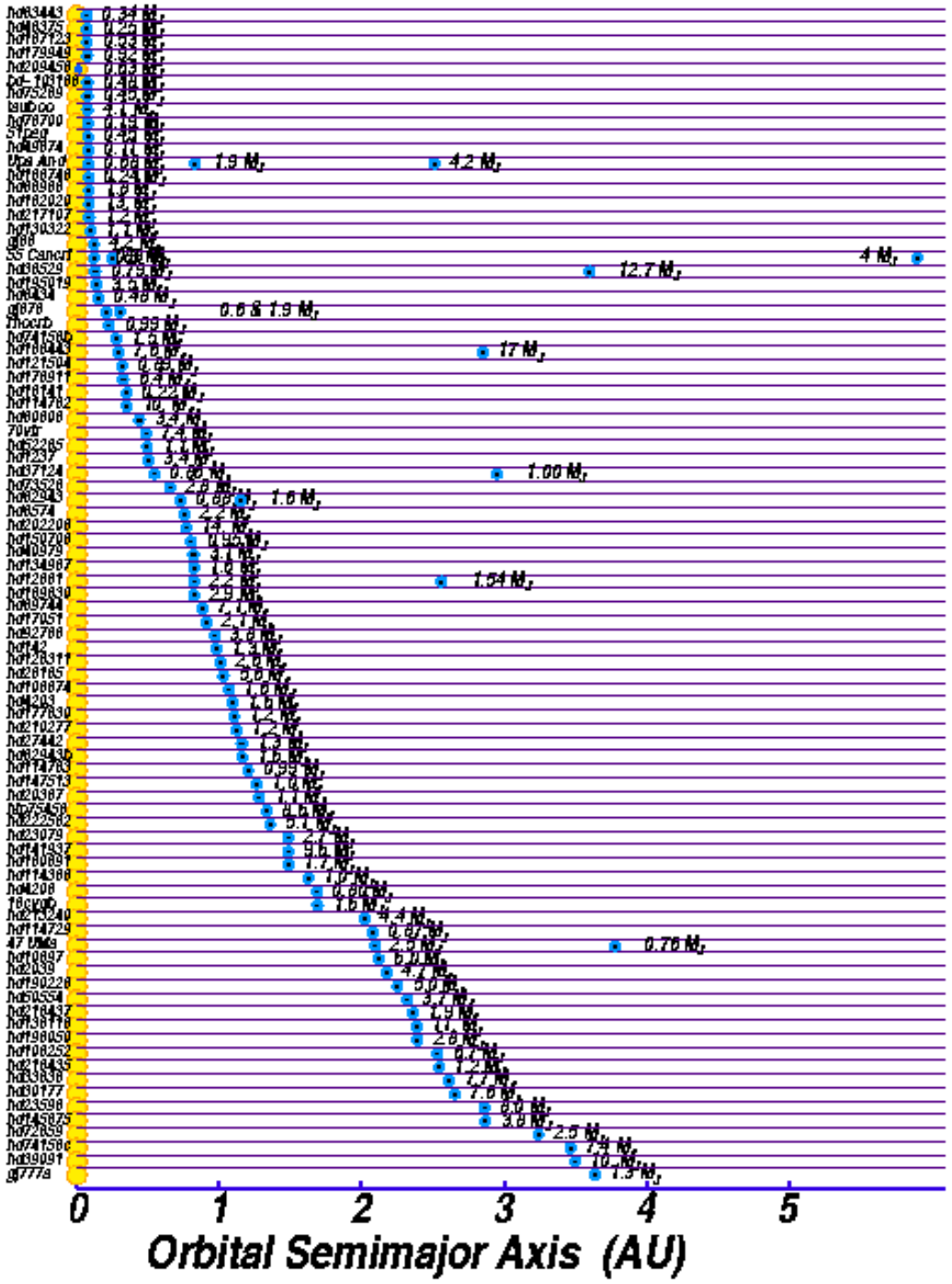

Planets found by Doppler Method

All Indirect Detections: only very recently has light been seen coming from the planets themselves.

Many planets are in very small orbits – “hot Jupiters”. These intercept a lot of light (IR radiation now detected by SPITZER) and may be detectable in reflected light..

The problem

- **For Hot Jupiters planet at least 10,000 times (10 mag) fainter than star and a few milli-arcsec away**

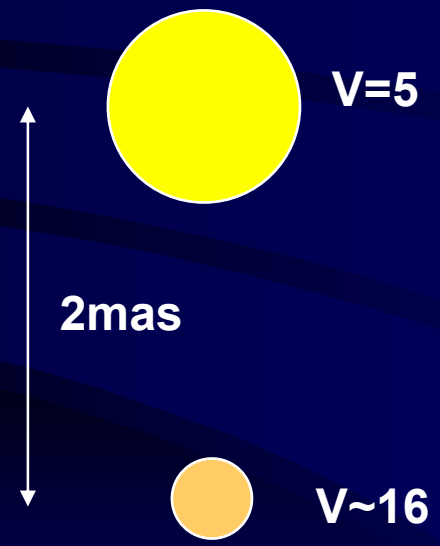

For other types of planets the angular distance from the star increases, but planet gets much fainter, as $1/r^2$.

Direct Detection methods for Hot Jupiters

- Spectroscopy
  - Look for weak doppler shifted spectral lines at velocity of planet.
  - Collier-Cameron et al. and Charbonneau et al. set upper limits on geometric albedo $p<0.4$ for Tau Boo and Upsilon And.
- Optical Photometry – reflected light
  - Look for change in brightness due to phase effect.
  - Requires very accurate photometry — probably not possible from the ground.
  - Observations from space should have sufficient accuracy - Canadian MOST microsatellite is trying to do this (Green et al. 2003, ApJ 597, 590)
    - Small (15cm) telescope so needs to combine many orbits.
    - 2.5 millimag variability detected (May 2005), indicating that the photometric modulation is dominated by tidal stirring of the star.

Thermal IR photometry – emitted light

- Two teams have recently used SPITZER to make the first direct detections of planets orbiting a sun-like star. Both groups observed transiting planets, picking up the drop in flux during the secondary eclipse.
- Deming et al.(2005, Nature 434, 740), used MIPS at 24 um to detect HD209458b.
- Charbonneau et al.(2005, ApJ 626, 523) used IRAC at 4.5 and 8.0 um to detect TrES-1. Teff=1060 K.

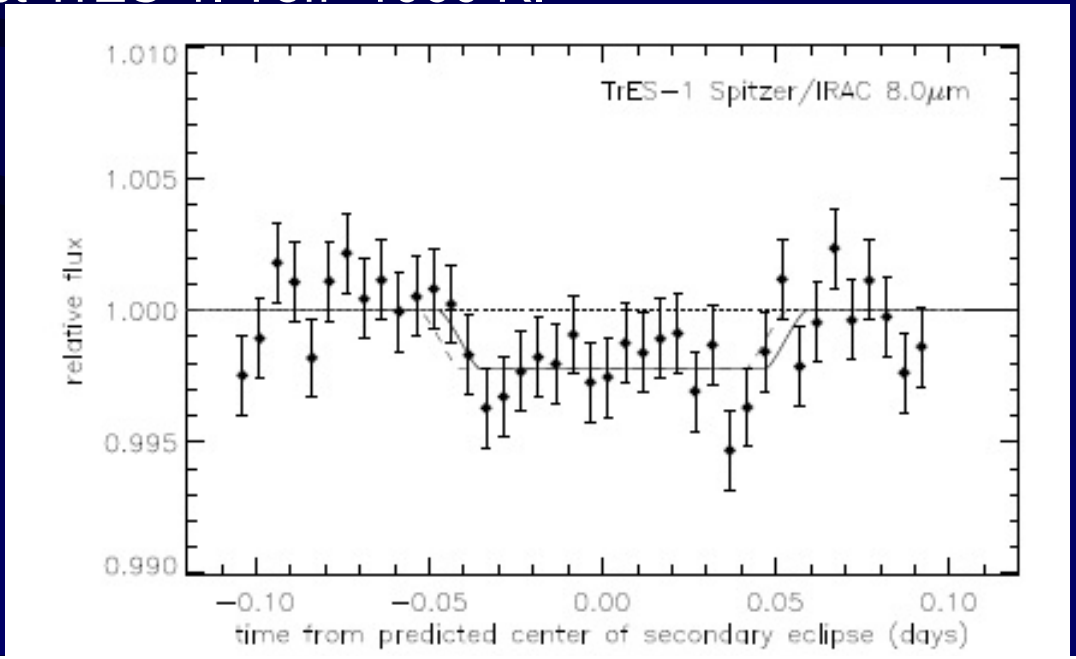

Polarimetric Method

- **Light from planet is polarized and polarization varies around orbit as scattering angle changes.**

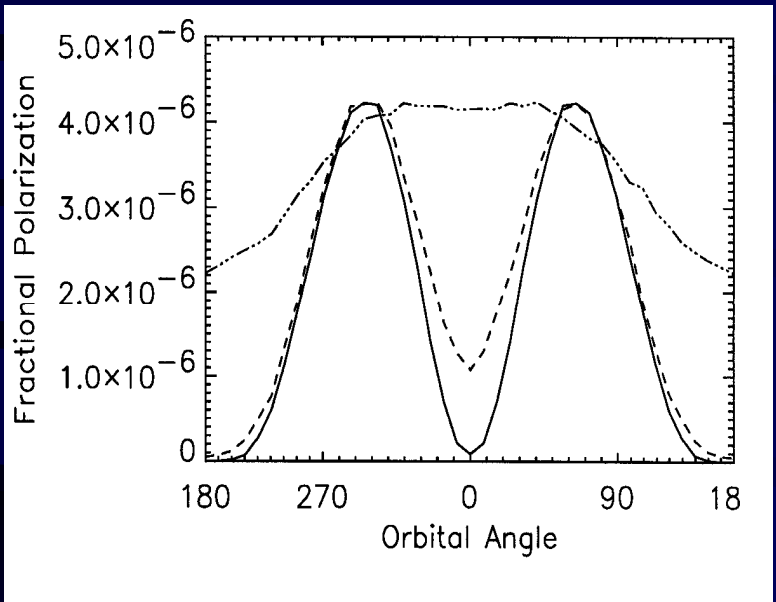

Seager, Whitney and Sasselov, 2000, Ap. J. 540, 504.

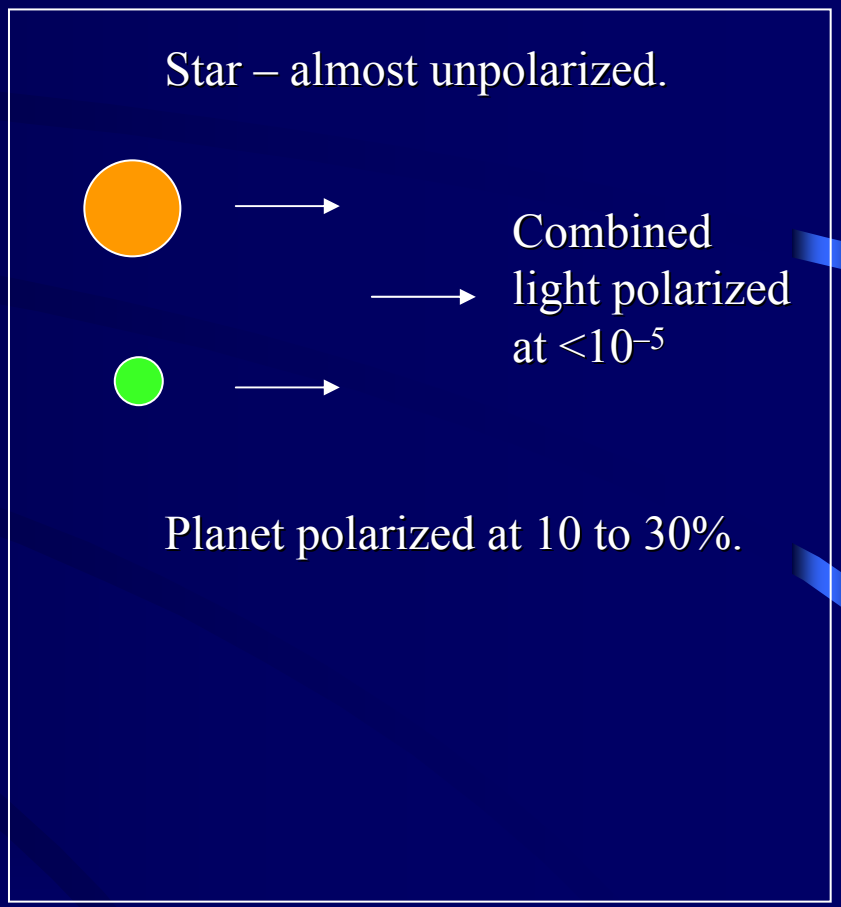

Polarimetric Method

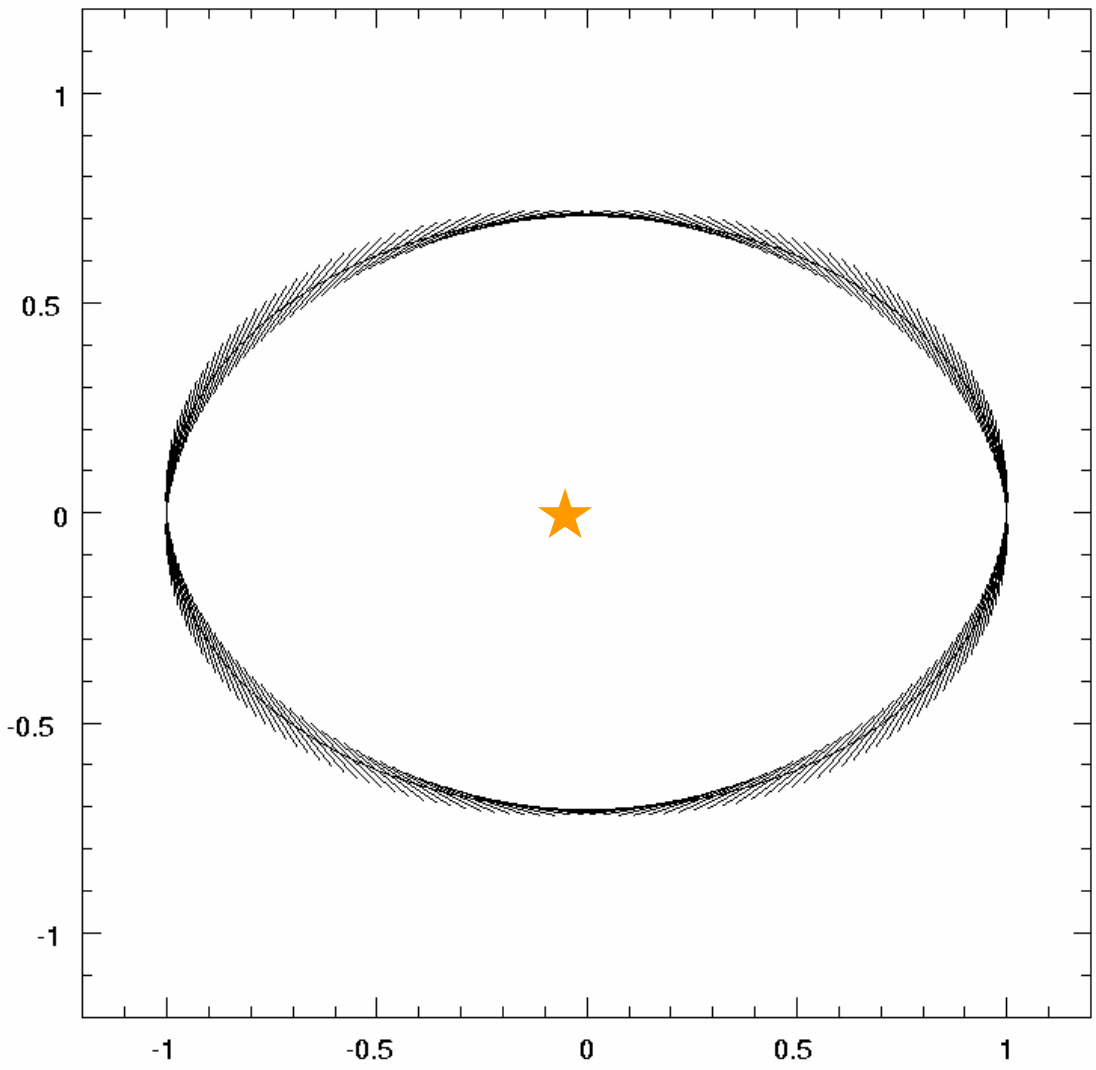

Stellar Polarisation

1) Stars are in fact weakly polarised at the limb, due to scattering by eg. electrons, protons, H^- ions. This polarisation is only a few parts in 10^4 at 780 nm.

- Averaged over the solar disc this polarisation is zero, unless the star rotates fast enough to be significantly oblate, in which case it will induce a constant polarisation. Tidal forces from the planet's gravity could have the same effect, but it is weaker.

2) Star spots are also linearly polarised at the 10^{-4} level and are circularly polarised at a higher level. The randomly oriented polarisations of different spots add in quadrature and will not produce measurable net polarisation unless the star is very active, in which case it should show jitter in the radial velocity surveys.

Planetary Signal in the QU Plane

The pol signal traces out a distinctive double loop in the QU plane, allowing the orbital phase to be identified despite any constant additional signal.

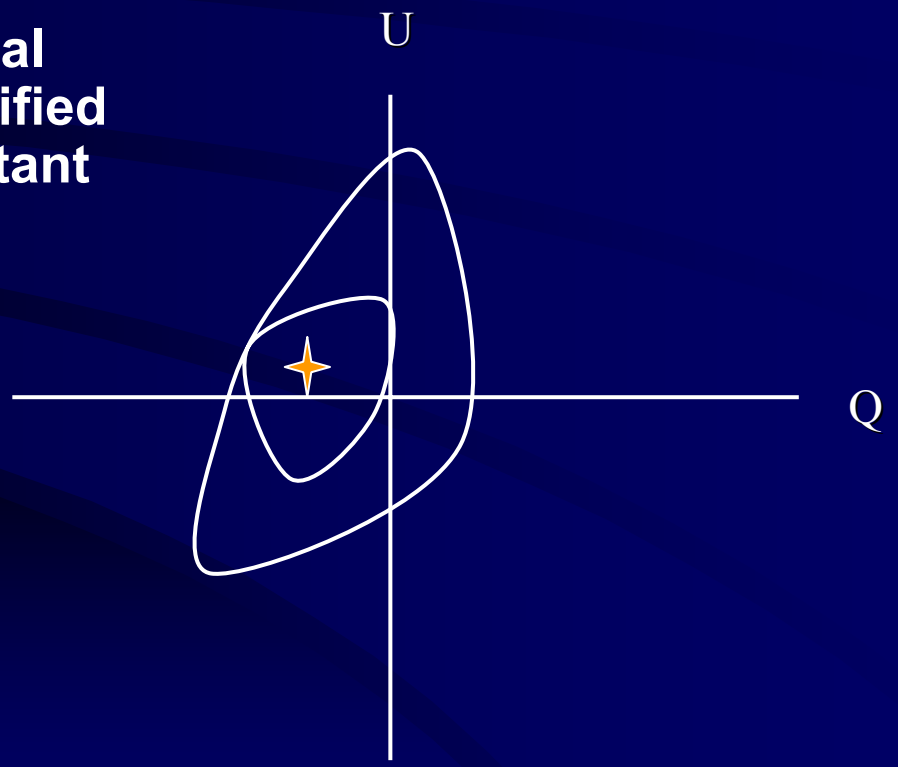

Possible Signals

- The magnitude and shape of the signal depends on orbital inclination, the composition and size of the scattering particles and the wavelength.
- Hence with good data we determine the Inclination (and hence mass), albedo in 3 colours, the nature of the scattering particles (Rayleigh or dust particles), planet radius and approximate temperature.

"…. Polarization signatures … are well under the current limits of detectability which is a few x 10^{-4} in fractional polarization" (Seager et al. 2000).

Seager, Whitney and Sasselov, 2000, Ap. J. 540, 504.

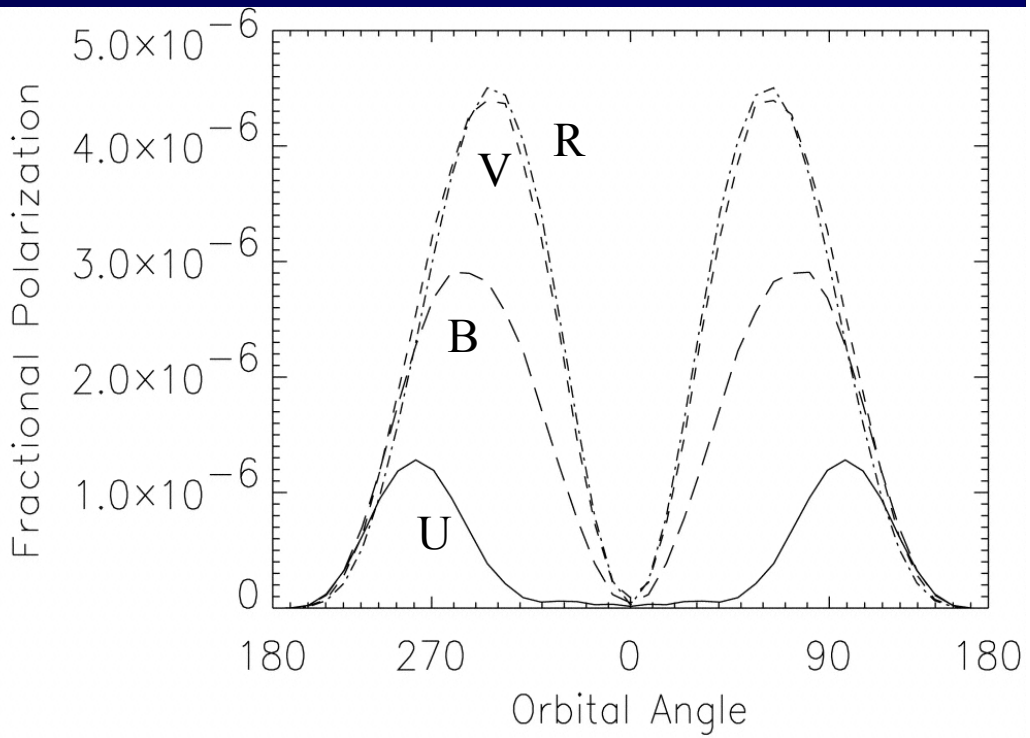

Possible Signals

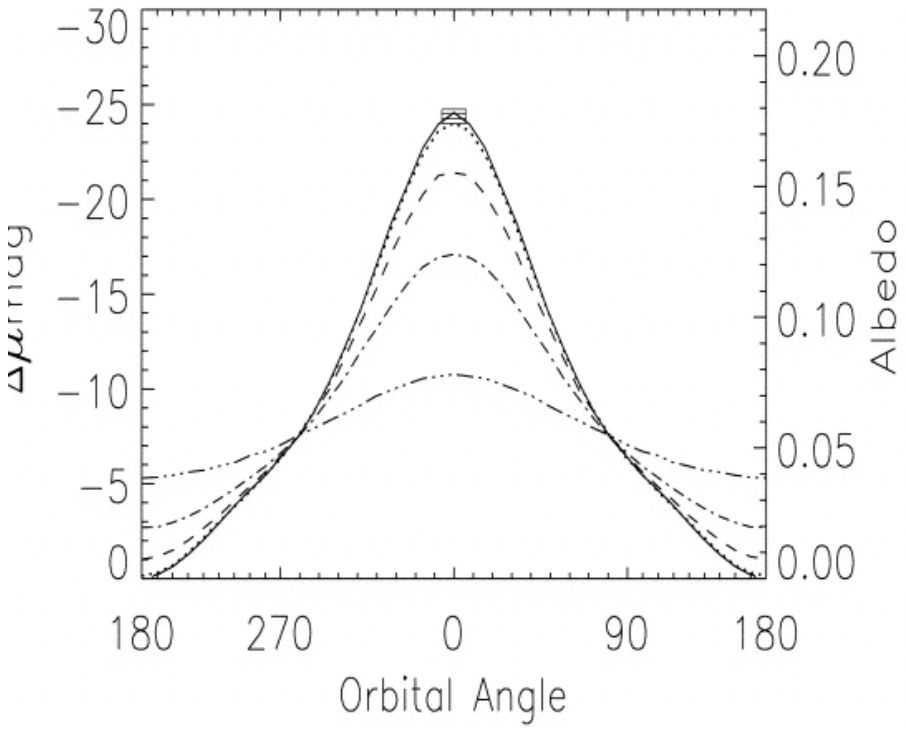

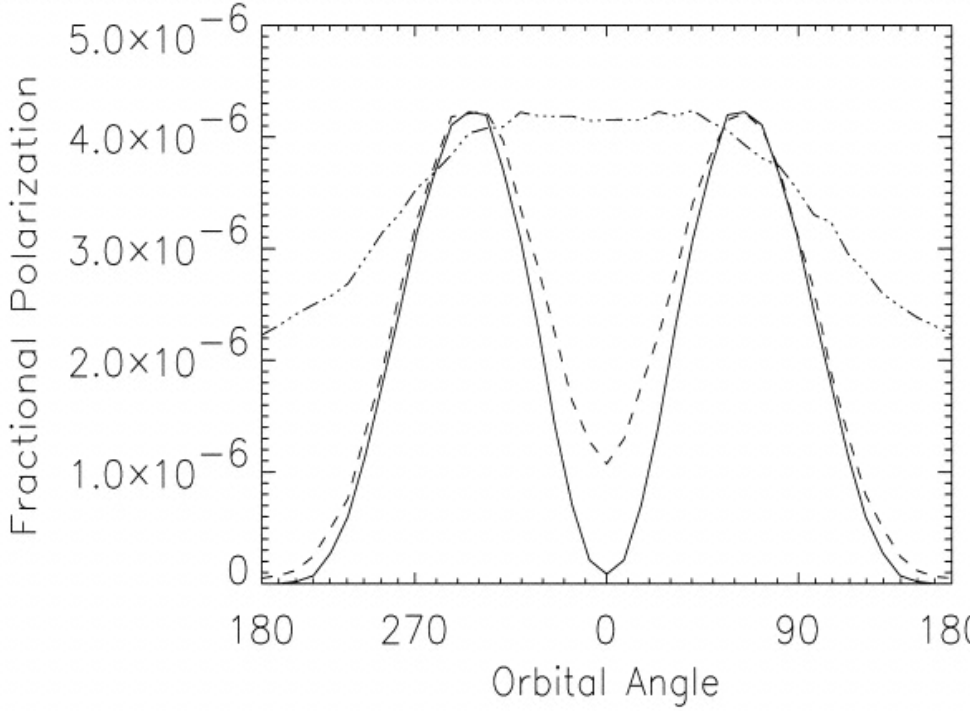

The optical polarization of the Sun measured at a sensitivity of parts in ten million

J. C. Kemp*, G. D. Henson*, C. T. Steiner*‡ & E. R. Powell†

* Department of Physics, University of Oregon, Eugene, Oregon 97403, USA
† Central Oregon Community College, Bend, Oregon 97701, USA

The integrated light of the Sun, an essentially spherical star with only slight asymmetries (small oblateness, weak overall magnetic field), would normally be found to be unpolarized, as observed in broad spectral bands with common instrumental sensitivities, 10^{-4}–10^{-5} fractional polarization[1–4]. Defining the Sun's intrinsic linear (LP) and circular (CP) polarizations down to much lower levels (10^{-7} or even 10^{-8}) would have consequences not only in solar physics but in other areas, setting, for example, a new standard for stellar polarimetry. We report measurements of the general polarization of the Sun, both CP and LP, over the whole disk and over large sectors, at an absolute sensitivity level of $\lesssim 3\times10^{-7}$, carried out during August–September 1986. Upper limits for the intrinsic whole-Sun LP from the best data (minimum Earth–atmospheric contamination) were 0.2×10^{-6} in the *V* (yellow) band and 0.8×10^{-6} in *B* (blue). Definite CP was discovered. (1) The

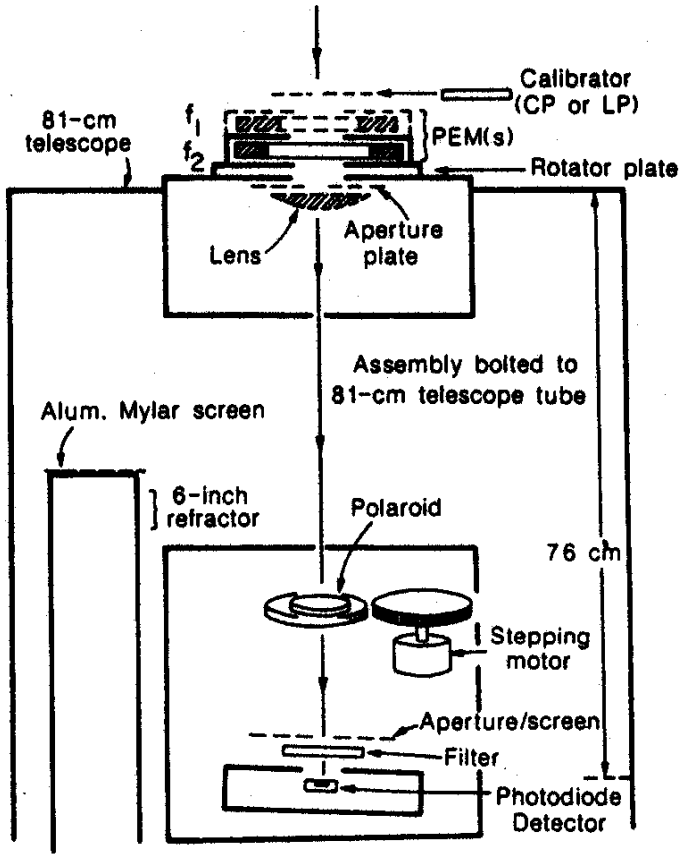

Fig. 1 Solar polarimeter assembly attached to the 81-cm telescope at Pine Mountain Observatory, Oregon. Telescope was used only as a solar spar, with entrance covered. Guiding was done with the 6-inch guide telescope, and by directly viewing the image on the

Polarimeters

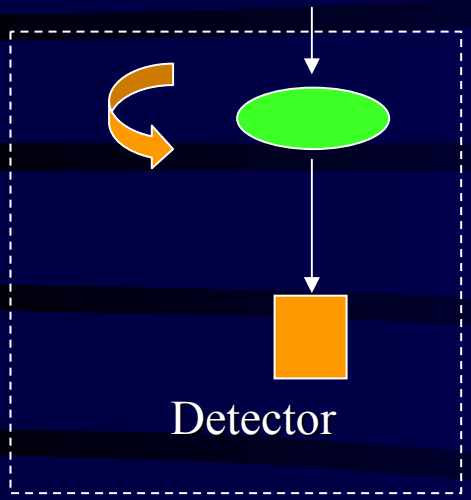

Rotating Polarizer

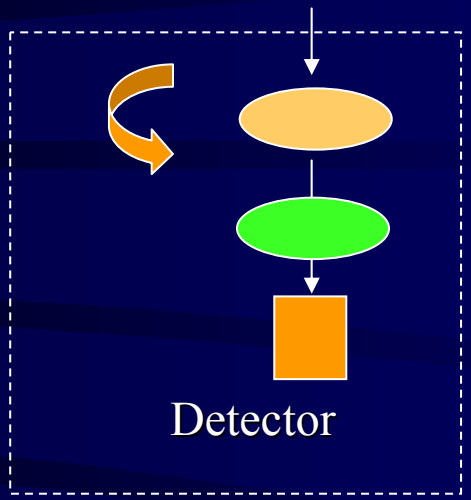

Rotating Retarder
(e.g. λ/2 plate)
Fixed Polarizer

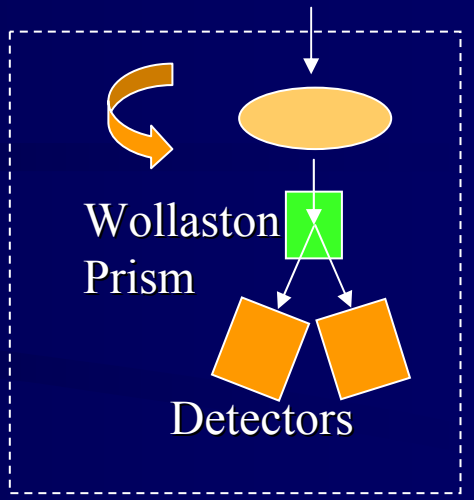

Rotating Retarder
Dual Beam System

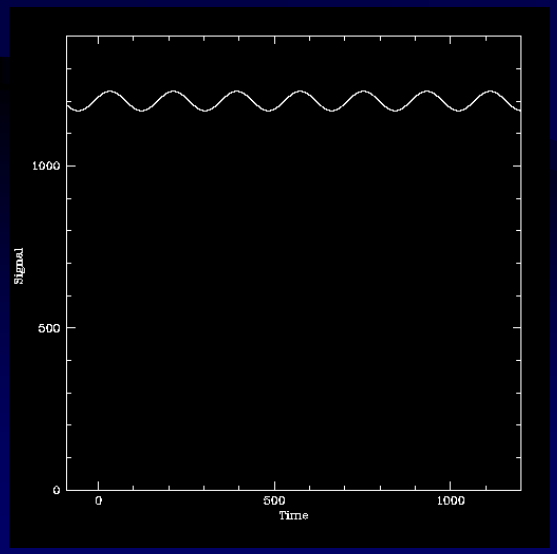

P

I

Disadvantages of Rotating Element Polarimeters

Single Beam systems: 2 measurements per Stokes parameter needed on a time scale similar to that of seeing effects and tracking errors. Dust on plate can give spurious modulation.

Dual Beam systems: A simultaneous differential measurement but it requires 2 different detectors and 2 measurements. Also requires high precision as well as high sensitivity. Image can move due to non-parallelism of the wavplate.

Photoelastic Modulators (PEMs)

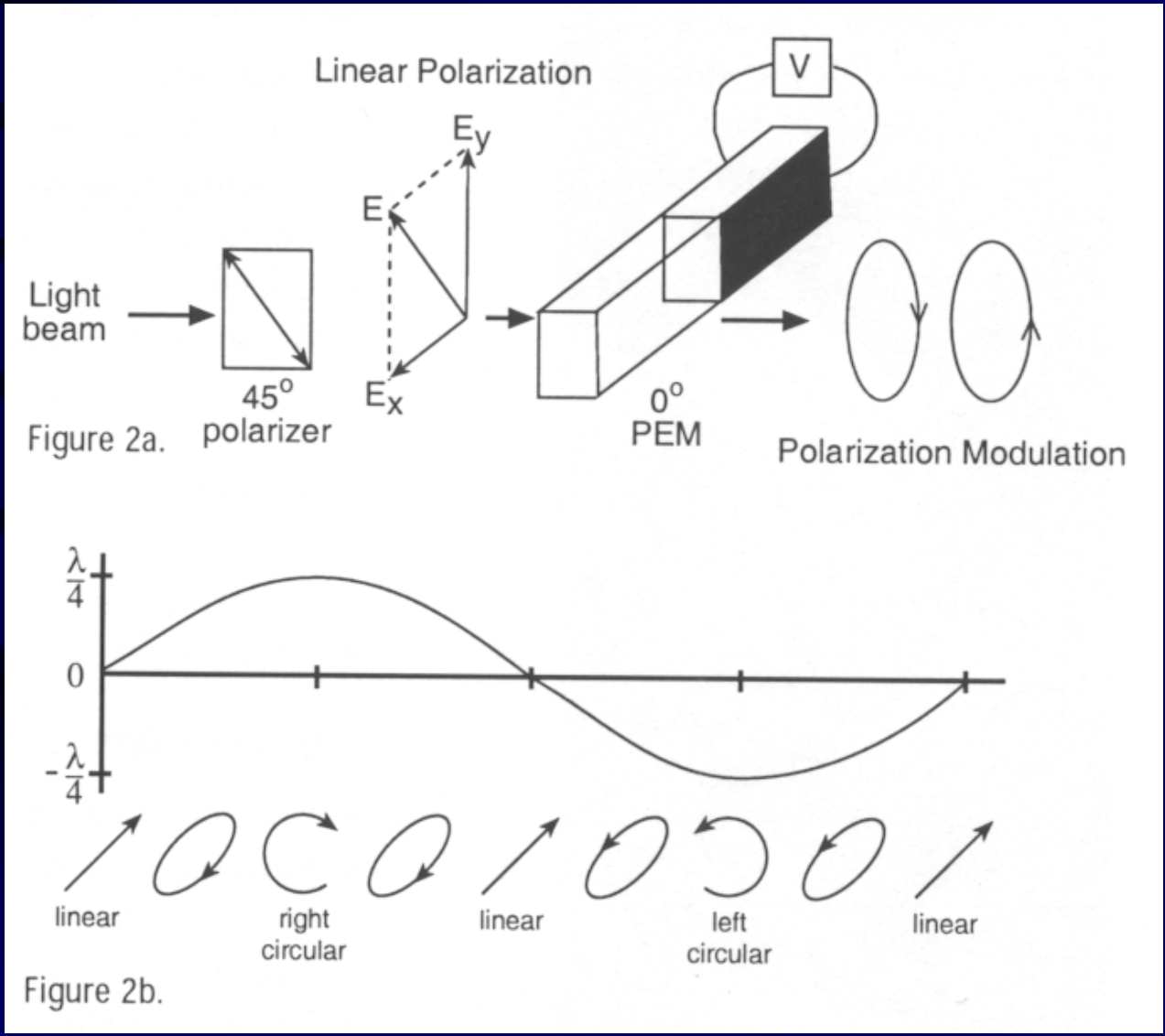

Photoelastic Modulators

HINDS INSTRUMENTS, INC.

PEM-90™ PHOTOELASTIC MODULATOR SYSTEMS

The signal falling on the detector is described by a Fourier series:

$$I(t) = I_0 + P_I \sin(2\theta)\sin(2\alpha)\{I_1\cos(2\omega t) + I_2\cos(4\omega t) + I_3\cos(6\omega t) + \ldots..\}$$

We detect the first overtone at 2ω with a Lock-in amplifier

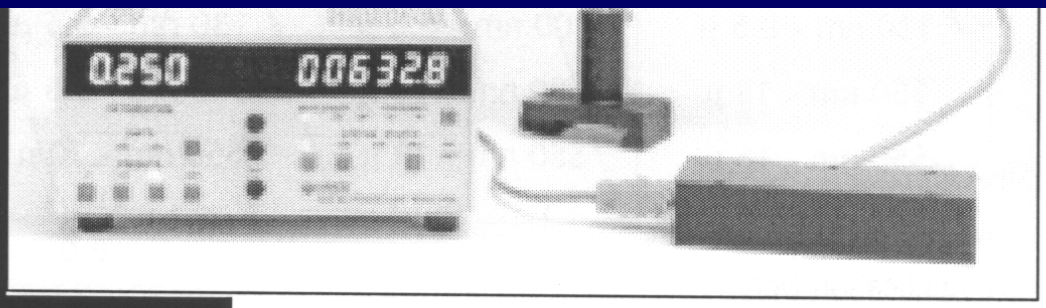

Figure 1.
Model I/FS50 PEM-90 photoelastic modulator with model PEM-90D controller.

closely-matched drive and control circuits to the PEM optics, Hinds Instruments has developed a range of photoelastic modulators for a variety of applications in a wide spectral region (UV to far-IR).

OVERVIEW OF FEATURES

- High sensitivity (10^{-6} or better)
- A resonant device generating a sinusoidal retardation at a fixed frequency

OPTICAL HEAD FEATURES

- Isotropic optic material
- Wide useful aperture (1.5 - 3.0 cm for standard models)
- Wide acceptance angle (±25°)

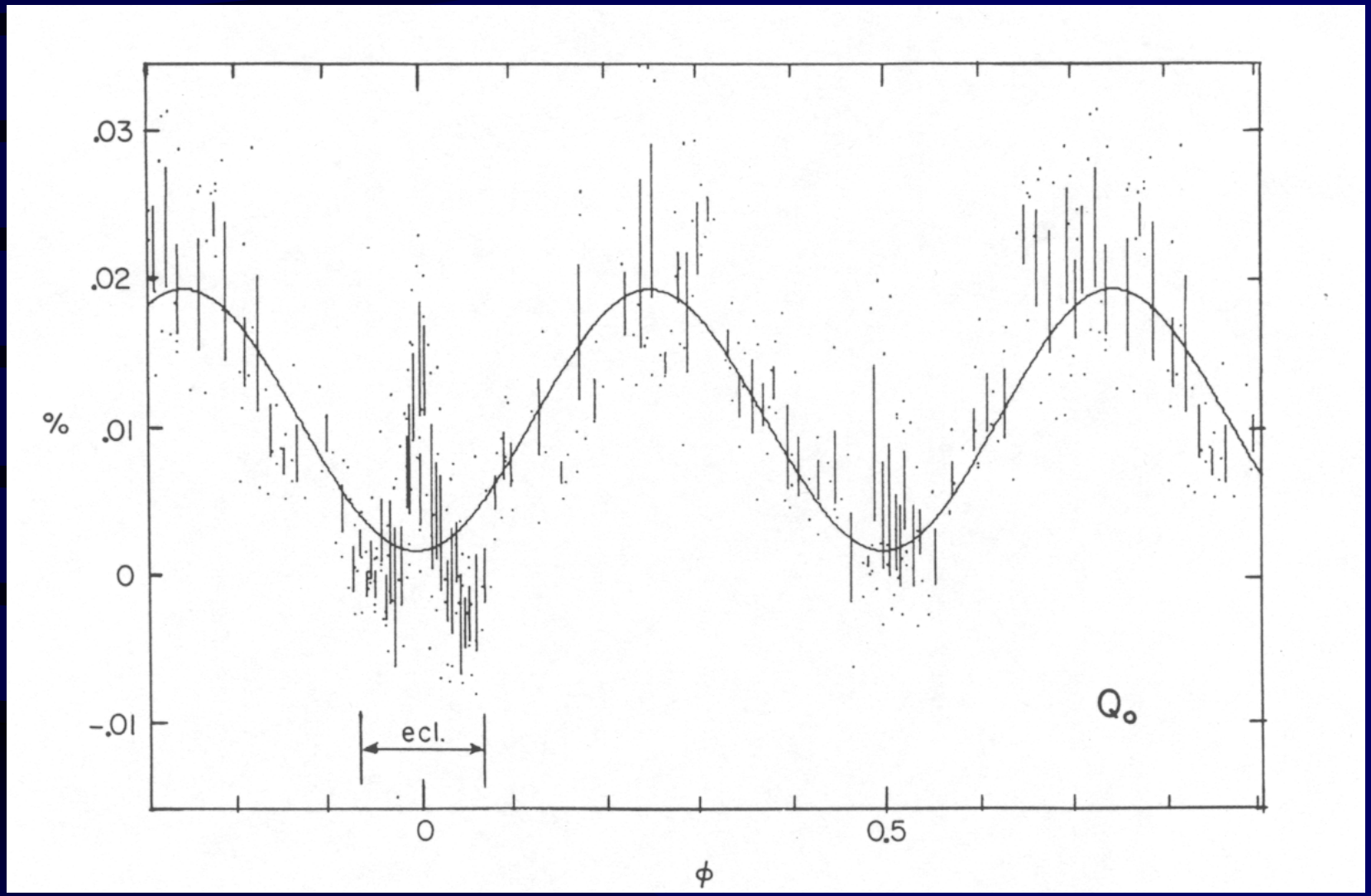

Polarization of Algol measured with Kemp's polarimeter at Pine Mountain Observatory - showing the "Chandrasekhar Effect" (1983)

Probably the most accurate stellar polarimetry prior to PLANETPOL.

Limitations on Sensitivity

10^8 photons	10^{-4} sensitivity
10^{10} photons	10^{-5} sensitivity
10^{12} photons	10^{-6} sensitivity
10^{14} photons	10^{-7} sensitivity

- CCD
  - typical well depth is ~200,000
  - Image spread over ~10 pixels
  - Need to combine 50 observations to get 10^{-4}
- Photon Counting Photomultiplier
  - Max count rate ~1MHz
  - In one hour can get to ~ a few x 10^{-5}
- Limitation on Polarization Sensitivity are set by Detectors conventionally used for astronomy.

Avalanche Photodiode Modules

- **Hamamatsu Photonics designed a custom APD module to meet our specs. It contains the APD (thermoelectrically cooled to –20C), power supply and preamplifier in a compact module**
  - **Frequency response DC – 70 kHz**
  - **Range 0.53pW (1.5 x 10^6 phot s^{-1}) to 26nW (7 x 10^{10} phot s^{-1})**
  - **NEP < 2fW $Hz^{-1/2}$**
  - **QE 75% at 0.7μm 50% at 0.5μm**

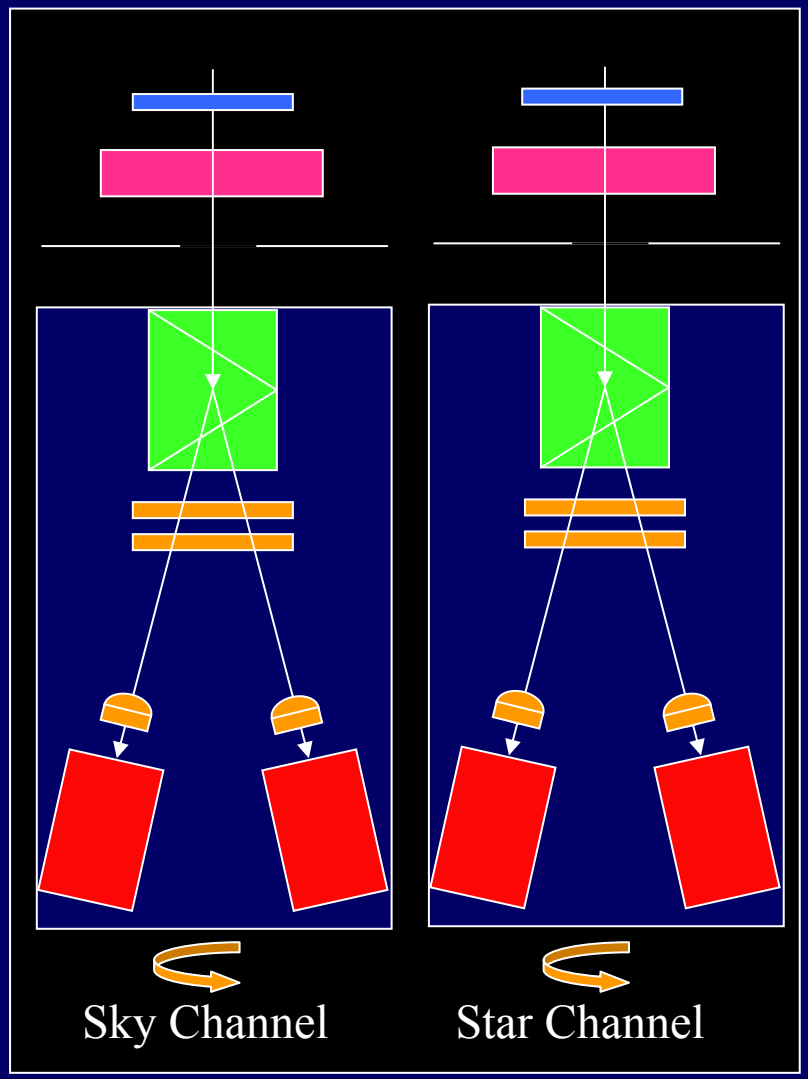

Calibration Slide

PEM

Aperture Wheel

Wollaston Prism
(3 wedge cemented)

Two Filter Wheels

Fabry Lenses

Avalanche Photodiode
Modules

Each channel (blue section)
rotates about its axis

Entire instrument rotates
about star channel axis

Signal Processing

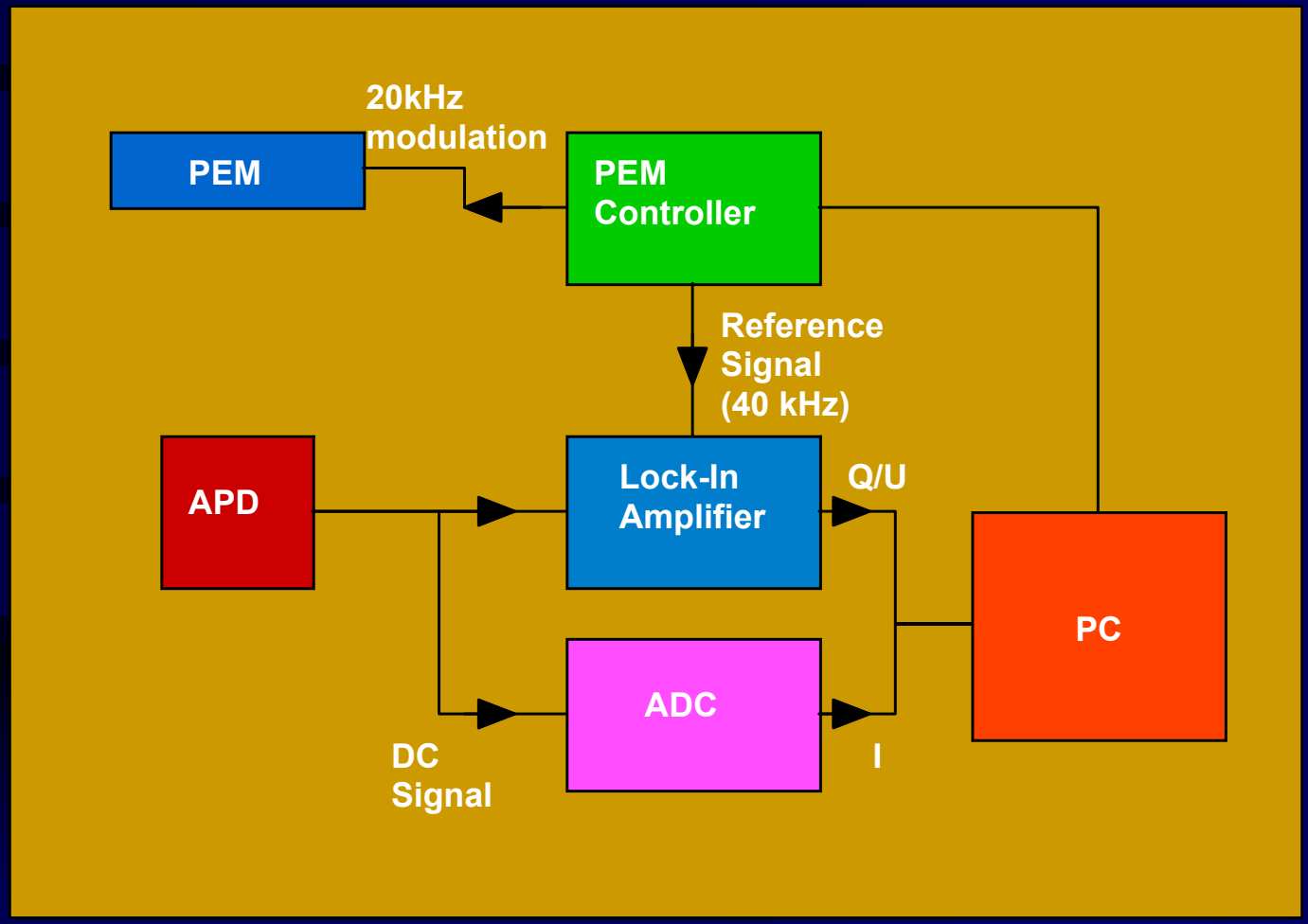


ALTURA LIBRE

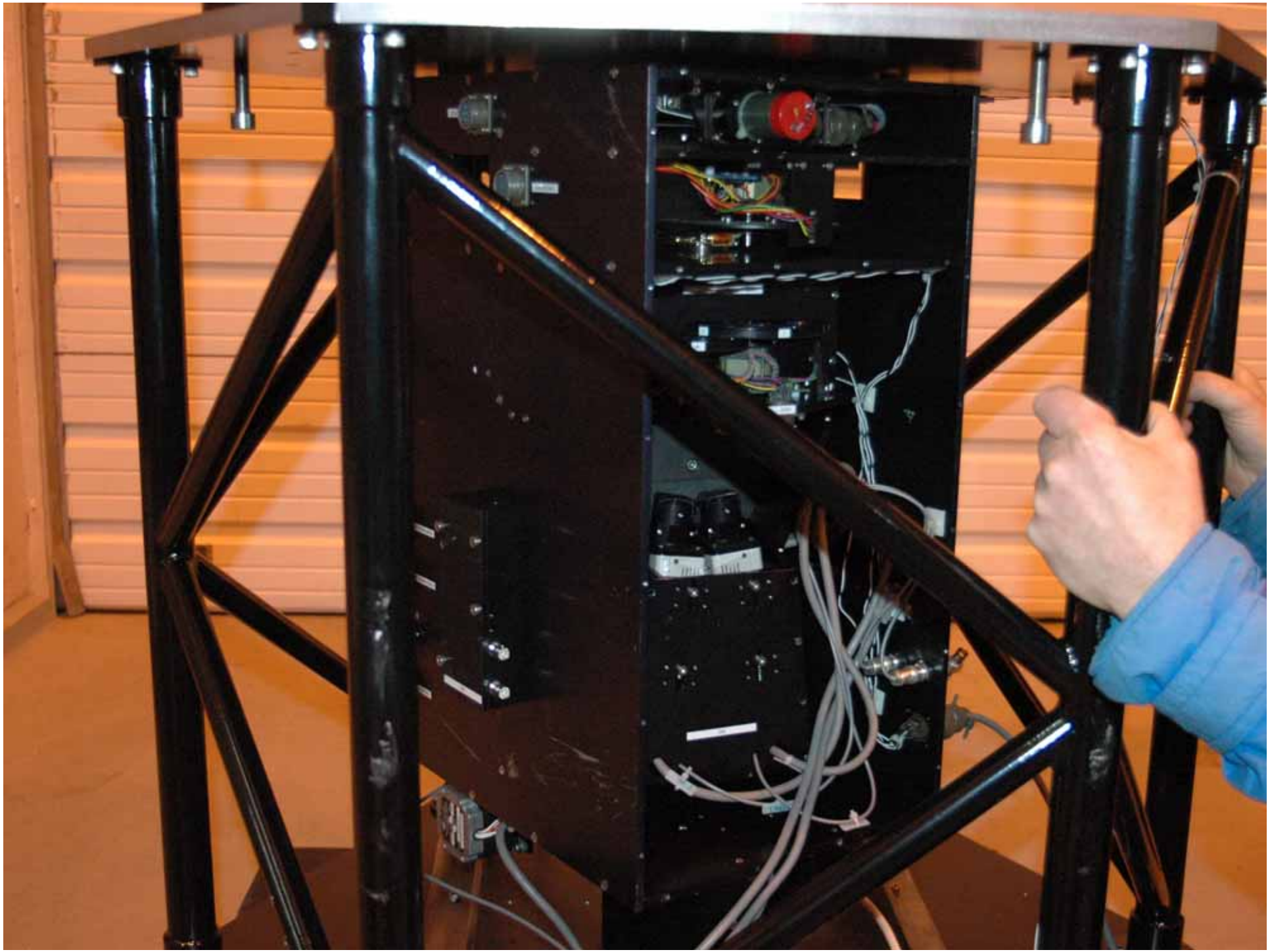

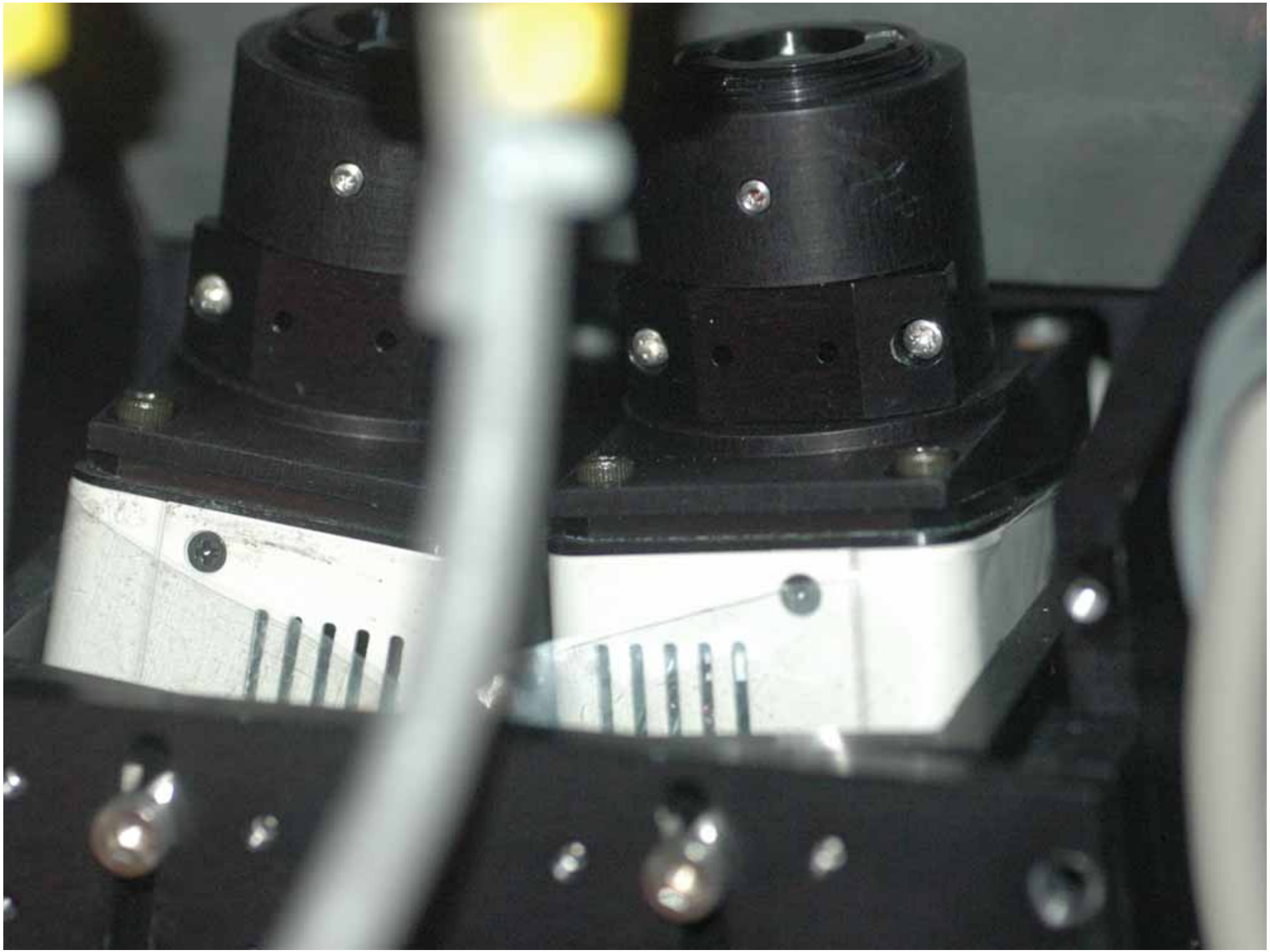

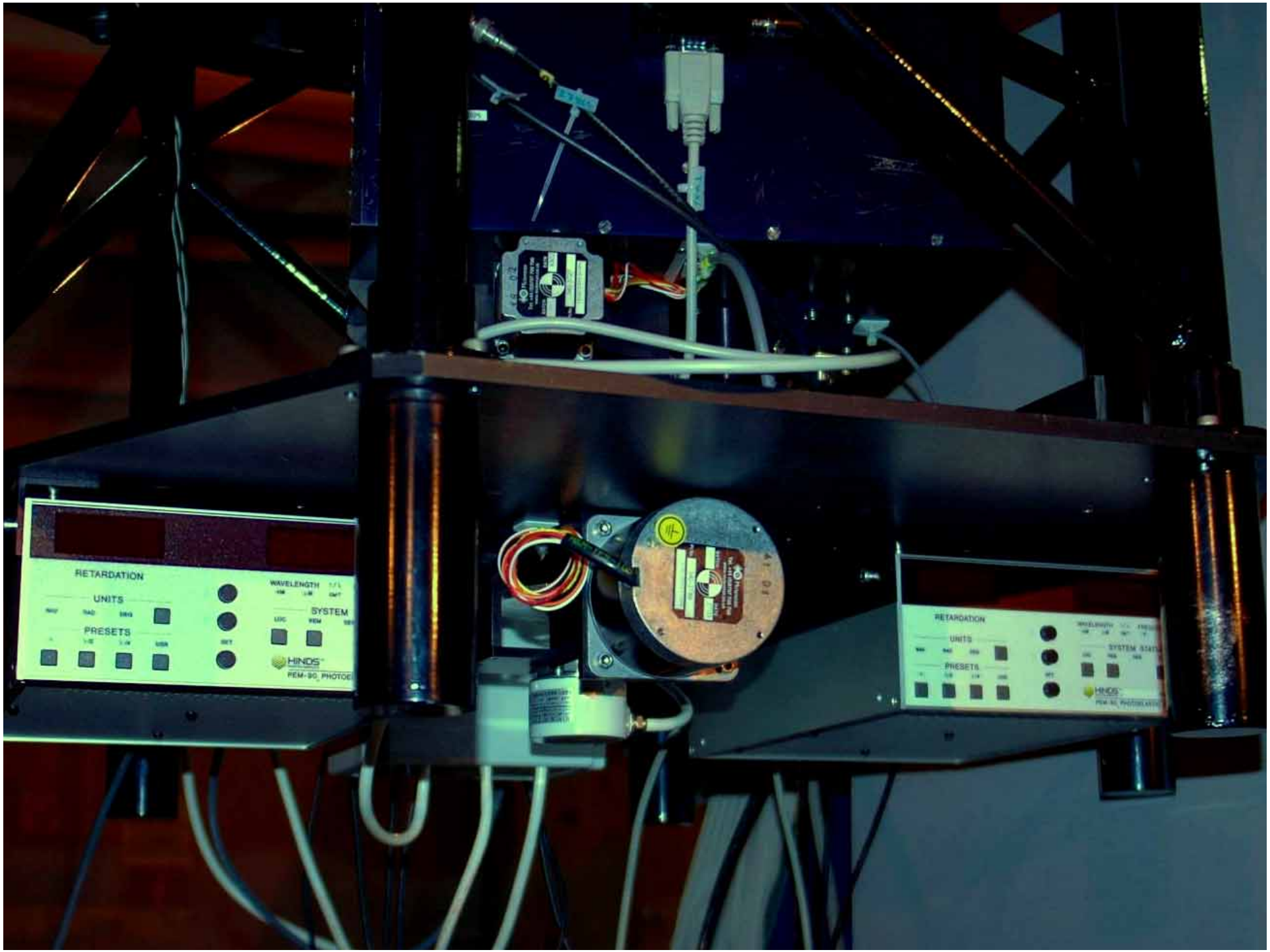
RETARDATION
UNITS
PRESETS
WAVELENGTH
SYSTEM
HINDS
RETARDATION
UNITS
PRESETS
HINDS


VEE Pro - ControlDataqADCTS17
File Edit View Debug Flow Device I/O DataAcq Data Display Window Help
Untitled
Start or Last Run
Fri 23/Apr/2004 23:43:14
Close slider Controls
Close Channel Rotation Controls
Close Instr Rotation Controls
Lockin Settings
Close Lockin Controls
Plots
Start Lock
Start Both
Start ADC
Close ADC Controls
Open PEM Controls
AUTO
No Entries
Step No
MANUAL
3
Close Controls
Plots & Data
UserFunction
LockinUOTS17
Star1 File
To File: C:\jhh\24AprStar1_5
Clear File At PreRun & Open
Star1
Clear
STAR1Chart
Y name
Trace1
Trace2
Step Size: 1
X name
Star2 File
To File: C:\jhh\24AprStar2_5
Clear File At PreRun & Open
Star2
Clear
STAR2Chart
Y name
Trace1
Trace2
Step Size: 1
X name
Sky1 File
To File: C:\jhh\24AprSky1_5
Clear File At PreRun & Open
Sky1
Clear
SKY1Chart
Y name
Trace1
Trace2
Step Size: 1
X name
Sky2 File
To File: C:\jhh\24AprSky2_5
Clear File At PreRun & Open
Sky2
Clear
SKY2 Chart
Y name
Trace1
Trace2
Step Size: 1
X name
FastChannelControlT
FastChan1
ChanPosition
-45
FastChan2
ChanPosition
-45
FastInstr1
45
ADCUOTS5
To File
To File: C:\jhh\24AprADC_5
Clear File At PreRun & Open
Clear
DC Levels
Y name
Star1
Star2
Sky1
Sky2
Step Size: 1
X name
Board Number
Rate
Low Channel
Range
+-1.25 VOLTS
High Channel
FrontBack

Observing with PLANETPOL

- **Telescope Polarization**
  - Normally measured by observing “unpolarized standard stars”.
  - However there weren’t any standards good to 10^{-6}.
- **Our Approach**
  - Only use unfolded Cassegrain focus (e.g. not Nasmyth).
  - Use Altazimuth mounted telescopes.
    - Telescope tube rotates relative to sky as a source tracks across the sky. This enables the telescope and star polarization to be separated.
    - Telescope Polarisation then has a sinusoidal modulation as a function of parallactic angle.

Observing with PLANETPOL 2

- **Instrument Polarization**
  - Any spurious polarization signal originating in the polarimeter itself.
- **Our Approach**
  - Minimized by PEM polarimeter design.
  - Dual beam system removes some spurious signals since they will be of opposite sign in the two beams.
  - "Second Stage Chopping" by rotating the "channels" (Wollaston plus twin detectors) from +45 degrees to –45 degrees relative to PEM reversing the sign of PEM modulation.
  - This removes an offset of about 10^{-5} in polarization, which are different in the 2 star channels.
  - Remaining Inst. Pol=2 x 10^{-6} and stable.

Observing with PLANETPOL 3

- **Sky Polarization**
  - **There is a significant polarized signal from the sky if the moon is up or any twilight is present.**
  - **We are observing bright stars but:**
    - **If Star is 5th magnitude**
    - **Polarization Modulation for 10^{-6} polarization is equivalent to 20th magnitude.**
    - **The sky can be very highly polarized (~50%).**
- **Solution**
  - **Instrument includes a sky channel which simultaneously monitors the sky.**
  - **Because photon noise in sky channel is much lower than in star channel, sky is measured very accurately and doesn't limit our S/N.**

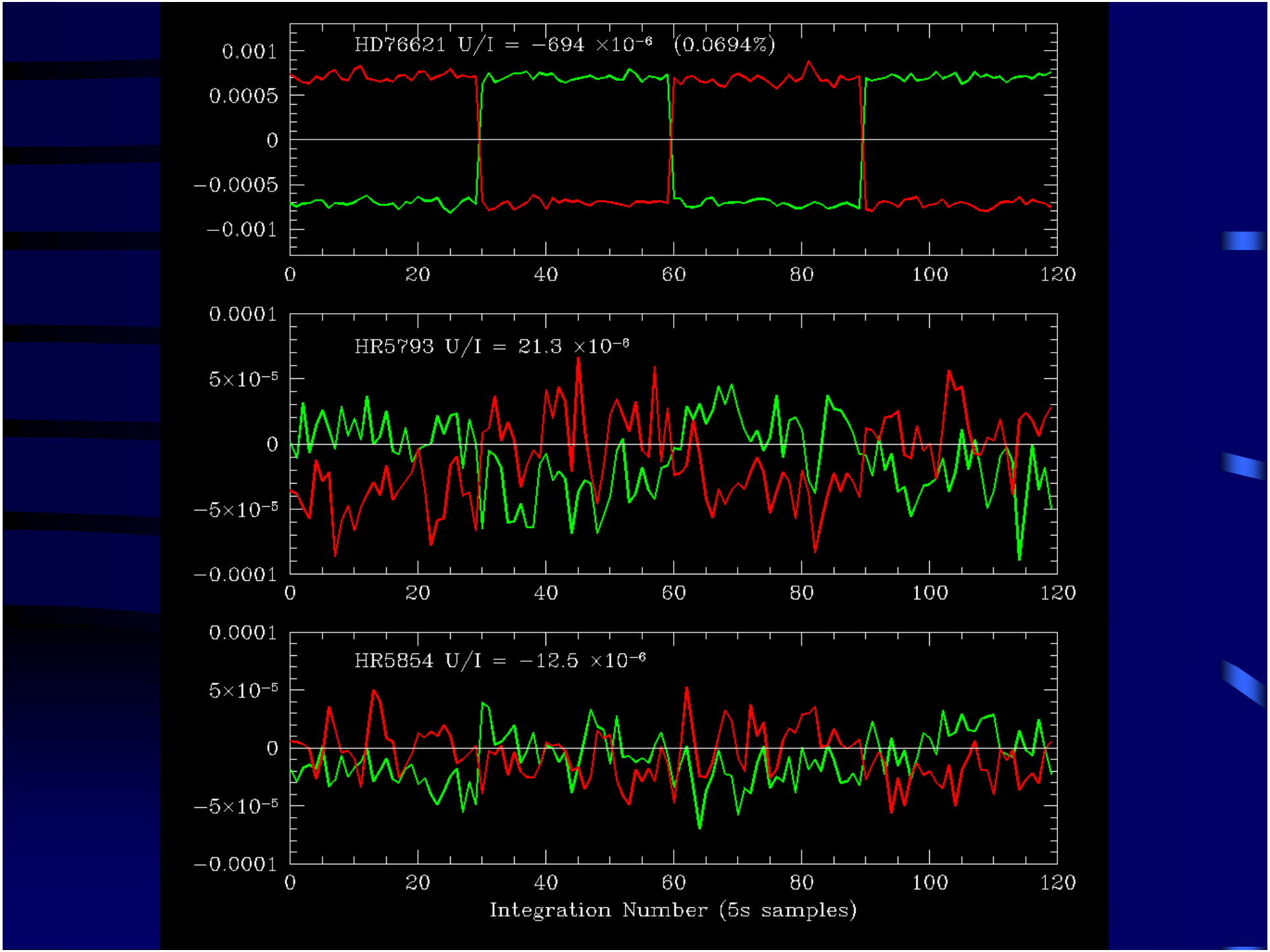
HD76621 U/I = −694 ×10⁻⁶ (0.0694%)
0.001
0.0005
0
−0.0005
−0.001
0
20
40
60
80
100
120
HR5793 U/I = 21.3 ×10⁻⁶
0.0001
5×10⁻⁵
0
−5×10⁻⁵
−0.0001
HR5854 U/I = −12.5 ×10⁻⁶
Integration Number (5s samples)

Tau Boo data – April 2004

- **During the April 2004 WHT run we measured the V=4.6 star τ Boo, one of our main candidates.**
  - **Errors of about 2.3 x 10^{-6} for each 24 minute measurement.**
  - **3 clear nights not sufficient for a definitive result.**
  - **More data was needed.**

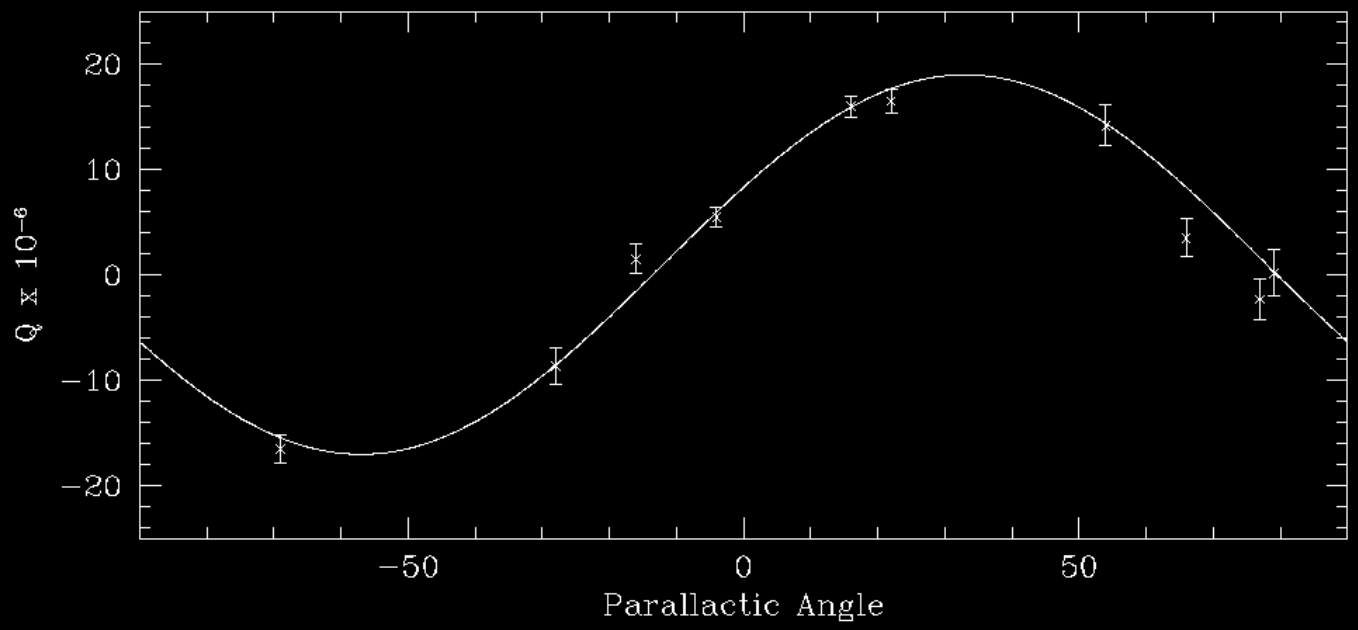
20
10
0
−10
−20
Q x 10⁻⁶
−50
0
50
Parallactic Angle

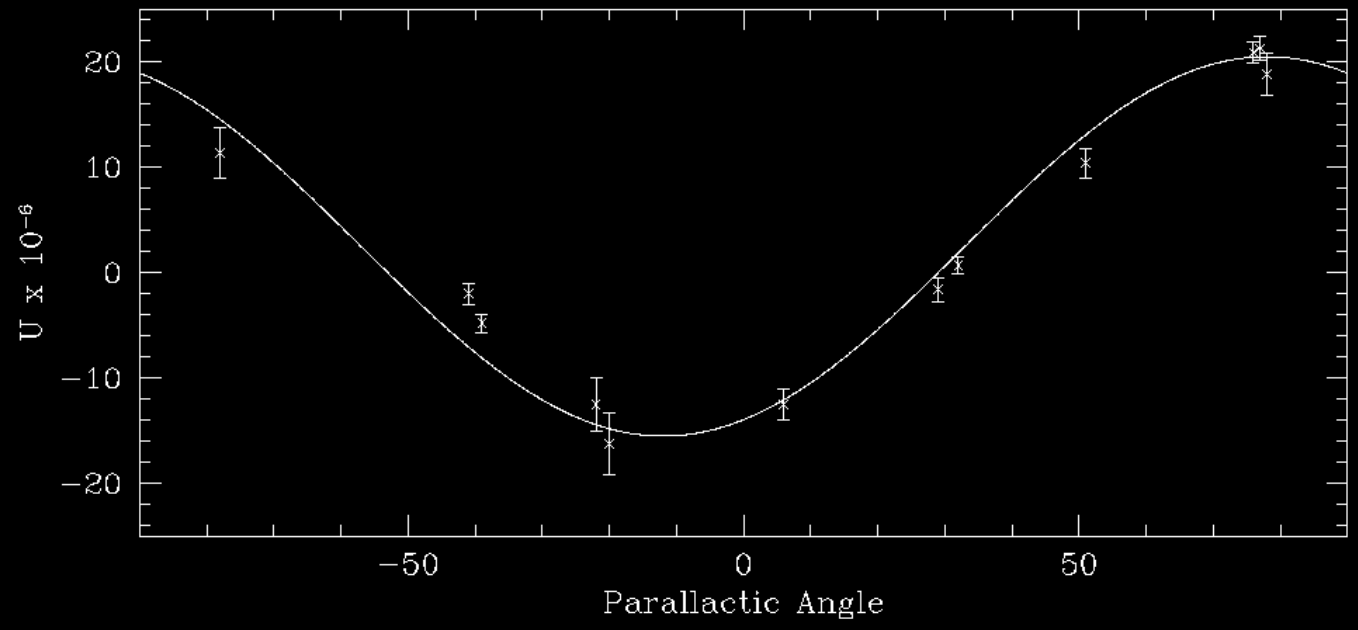
20
10
0
−10
−20
U x 10⁻⁶
−50
0
50
Parallactic Angle

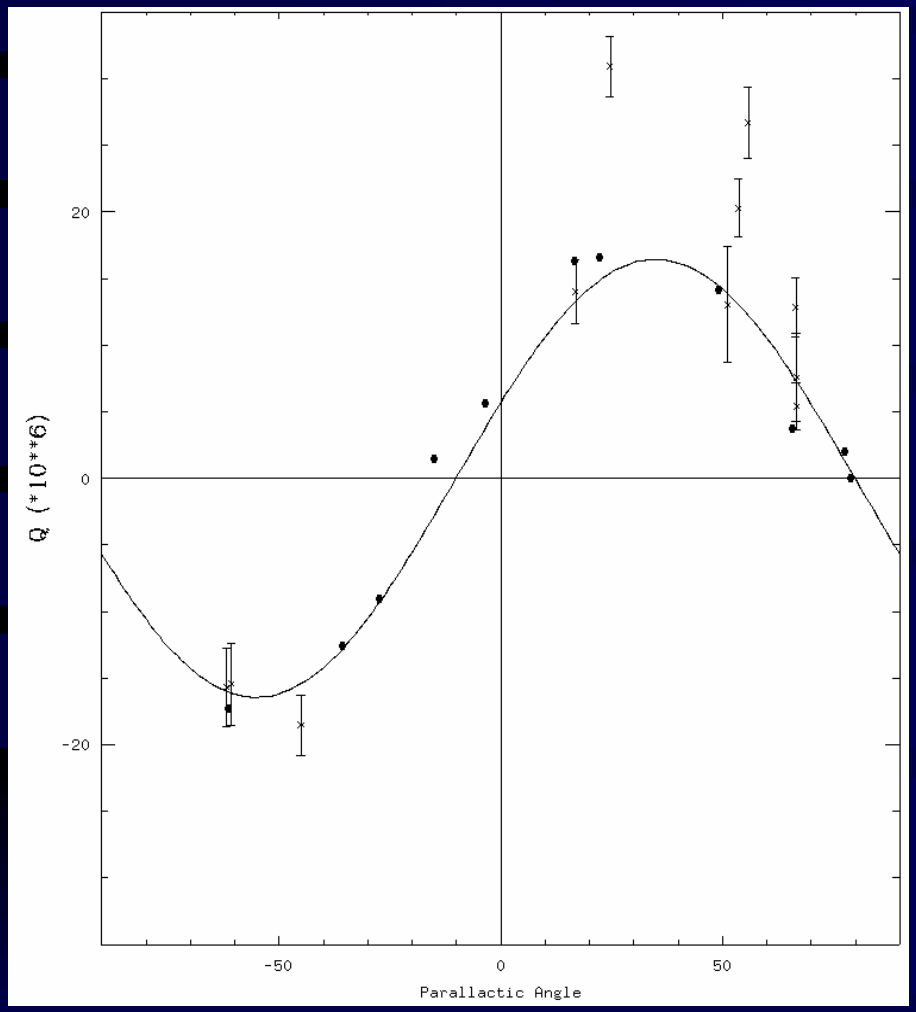
Q (*10**6)
20
0
-20
-50
0
50
Parallactic Angle

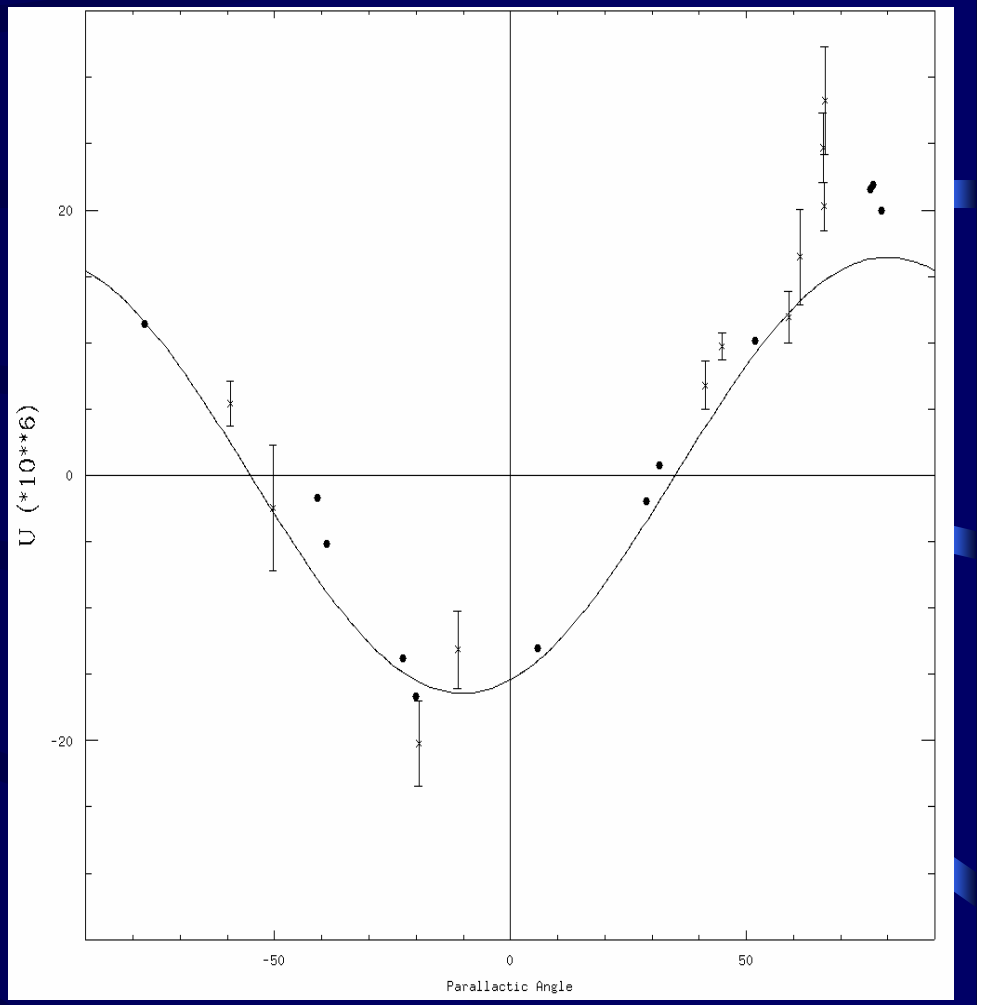
U (*10**6)
20
0
-20
-50
0
50
Parallactic Angle

Residuals for Tau Boo

Q

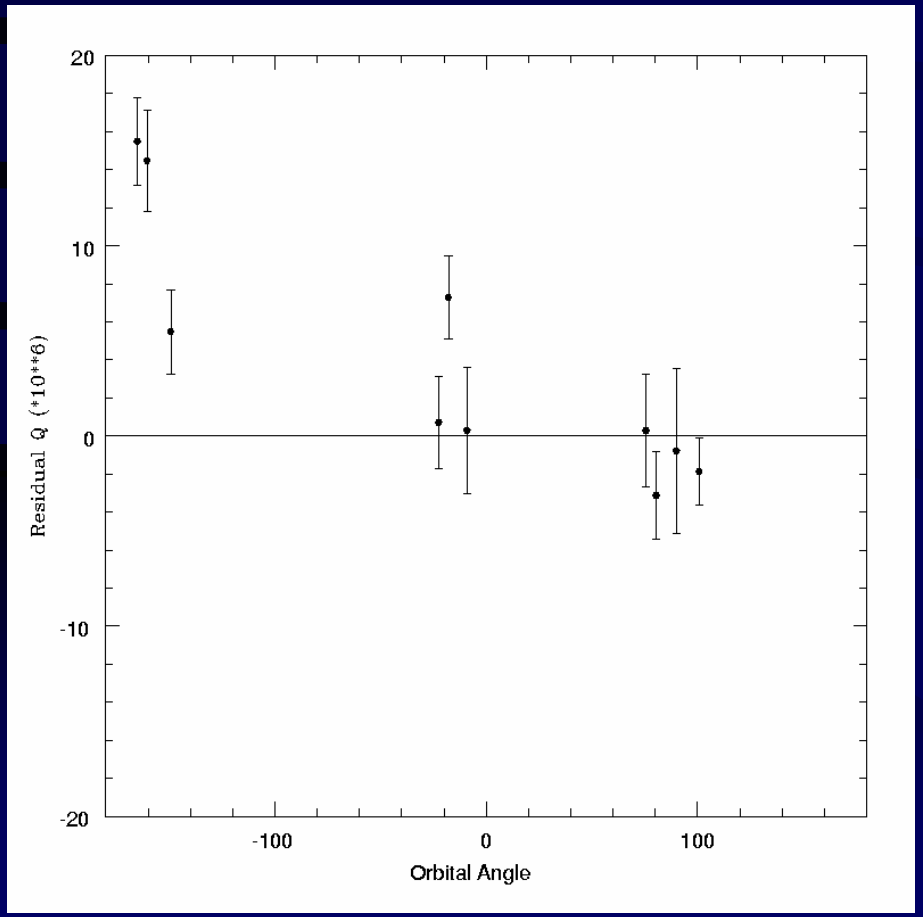

U

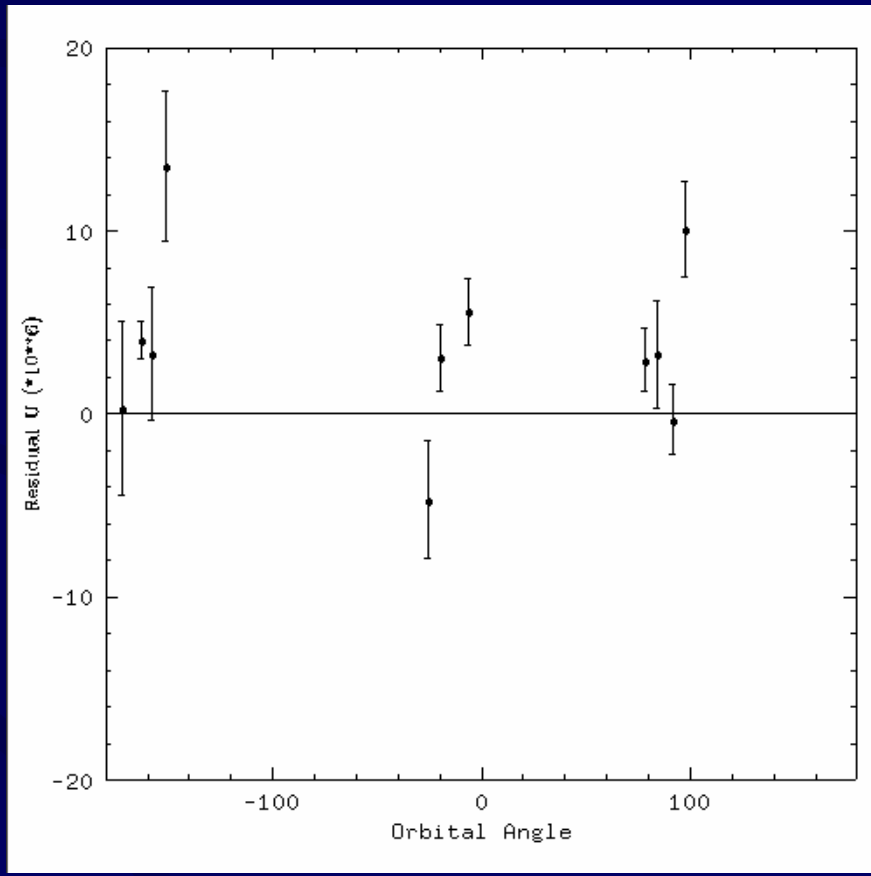

"Unpolarized" Stars

Star	Q/I (10^{-6})	U/I (10^{-6})
HR 5854 (α Ser, K2IIIb, V=2.6, 22pc)	0.44 ± 0.53	2.56 ± 1.76
HR 5793 (α CrB, A0V, V = 2.2, 22pc)	–1.50 ± 1.11	1.60 ± 0.93
HD 102870 (β Vir, F8V, V = 3.6, 11pc)	1.26 ± 0.94	3.19 ± 1.93
Procyon (α CMi, F5IV-V, V = 0.4, 3.5pc)	4.5 ± 3.0	–0.1 ± 2.3
HR 6075 (ε_2 Oph, G9.5IIIb, V = 3.2, 33pc)	45.4 ± 1.3	–5.7 ± 2.3

Polarized Stars

Star	Q/I (10^{-6})	U/I (10^{-6})
HD 76621	28.7 ± 3.0	–710 ± 2.7
u Her (Eclipsing binary)	102.4 ± 6.8	–169.0 ± 7.3
U Sge (Eclipsing binary)	–1362 ± 10	1274 ± 10
HD 187929 (Standard P = 1.8%)	3074 ± 4	–12734 ± 20
HD 198478 (Standard P = 2.8%)	4819 ± 25	20132 ± 164

Key System Features for Planet Detection

- **PLANETPOL works and delivers repeatable polarization measurements at the 10^{-6} level.**
- **The telescope polarization of the WHT is low and stable over a period of several days at least.**
  - **Good news - It could be much more difficult to get reliable results in the presence of a telescope polarization at the 10^{-3} to 10^{-4} level.**
- **Most normal nearby stars have very low polarization (0 - 10 x 10^{-6}).**
  - **Also good for the same reason: less precision is required than we had expected.**

October 2004 run – υ And

- **υ And is the brightest exoplanetary system (V=4.1).**
- **It has 3 known planets at 0.059 AU, 0.83AU and 2.5 AU.**
- **The masses are: 0.69 M_{Jup}, 1.89M_{Jup}, 3.75M_{Jup}**

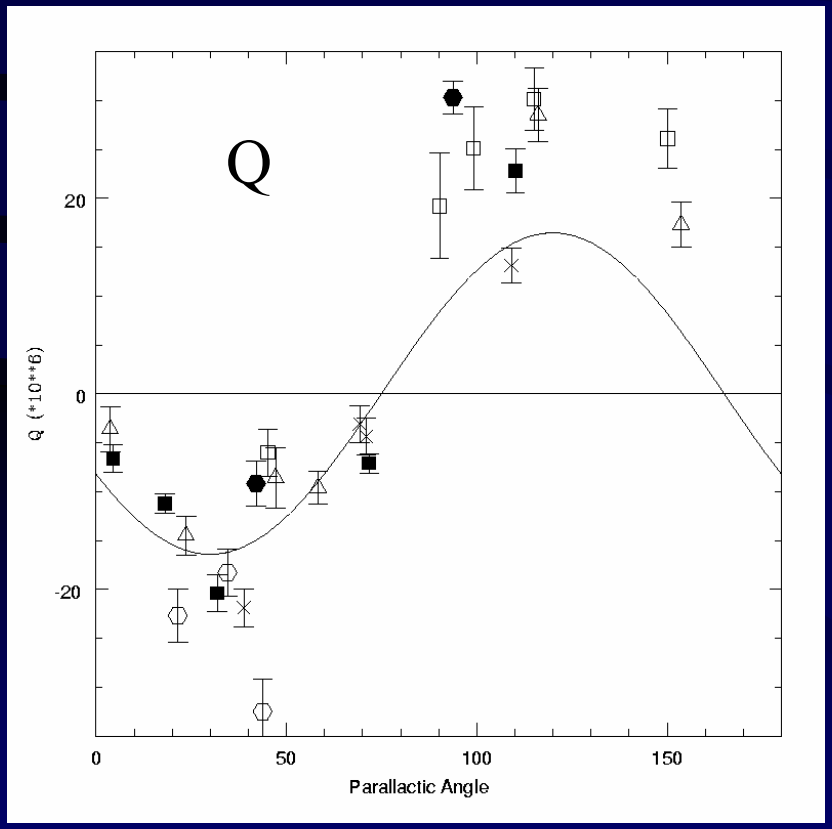

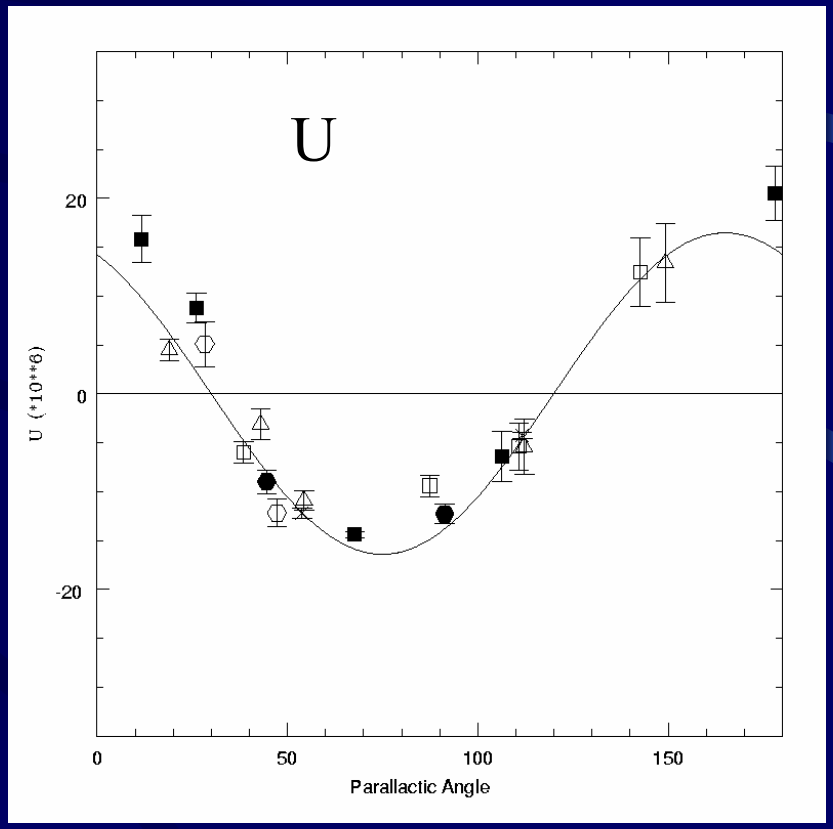

υ And – fitting the data

The Q and U plots show the data for 4 standard stars (large points) after fitting and subtracting the interstellar Pol for each star. The υ And data (small filled dots) are simply plotted without any modification.

All standard star data points are simultaneous fitted using Gauss-Newton minimisation of the squared errors.

Fitting Model: $Q = TP \cos(2(pa-x)) + q_i$ $\quad U = TP \sin(2(pa-x) + u_i$

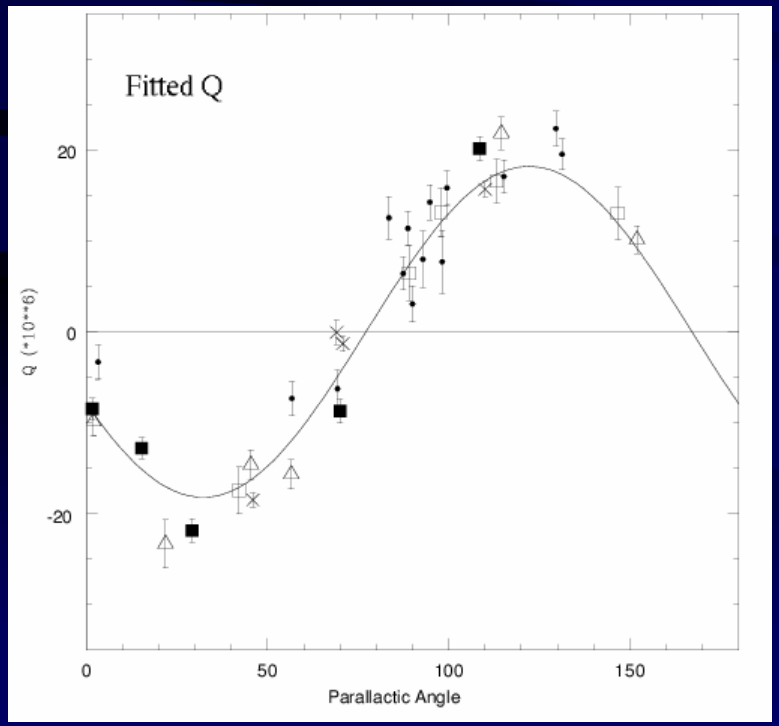

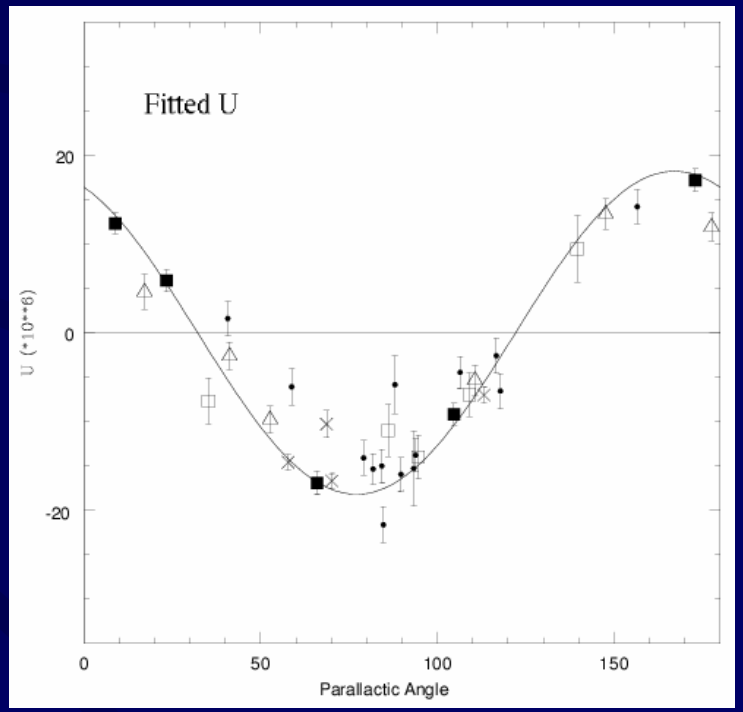

Tau Boo – Apr/May 2005

- **From 25-30 April we had mostly good weather and obtained the following data:**

From 3-9 May we had much worse weather but obtained some useful data on May 8 and perhaps also May 6 &7…..

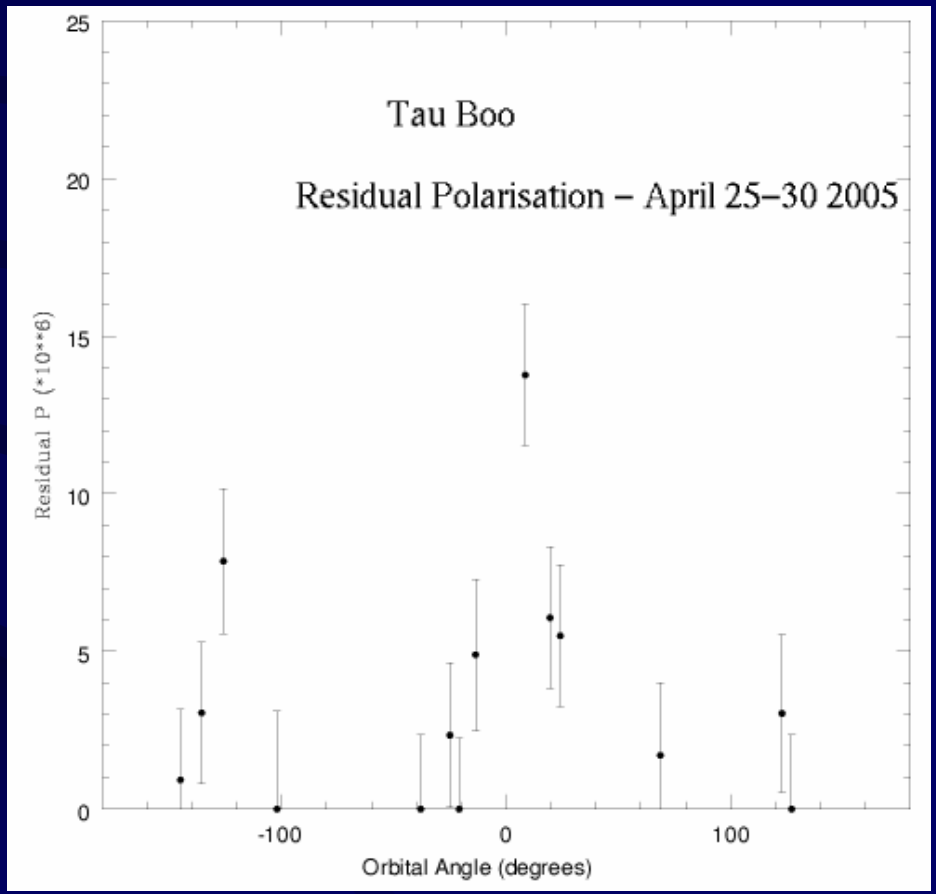

τ Boötis

MOST photometry – from a talk by Jaymie Matthews at the May StSci meeting.

- 11 days of observation in 2004
- ongoing observations a year later (now!)

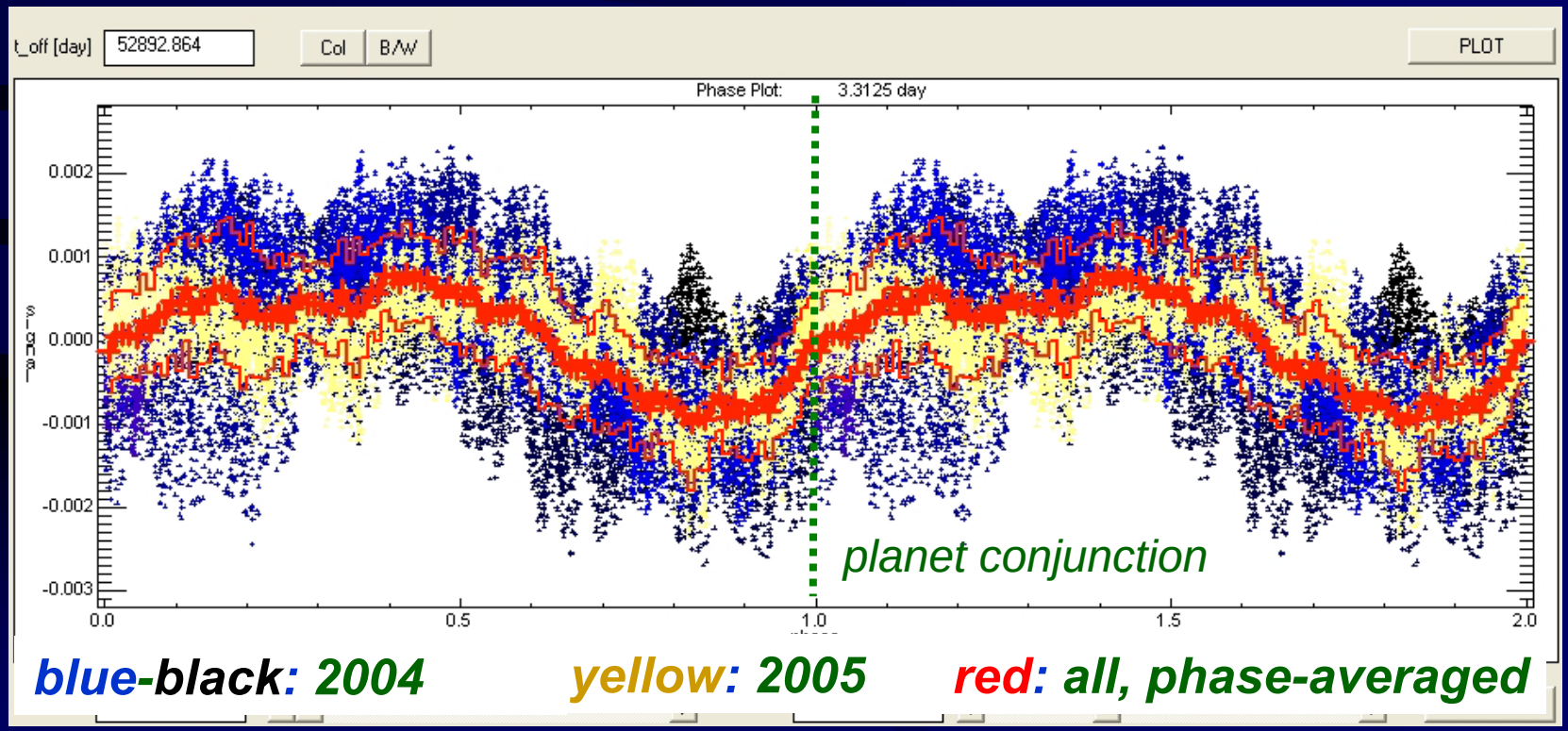

P_{RV} = 3.3125 d

(from Jaymie Matthews talk at StSci)

τ Boötis

- active young star?
  - stellar modulation period = planet orbital period
    - relatively large spot complex, like κ^1 Ceti, or travelling wave, induced by planet?
    - phase of stellar light minimum leads planetary conjunction by ~0.1-0.2 cycles
    - irregular variations from cycle to cycle
  - stellar envelope spun up by planet?
    - "rejuvenated"?
- effects on RV measurements?
- photometric detection of planet reflected light difficult

(from Jaymie Matthew's talk) at StSci

Transiting exoplanet system – HD209458b

- phase diagram of 7 days of photometry
  - P = 3.52474895 ± 0.00000096 d
  - upper limit on eclipse depth ~ 50 ppm

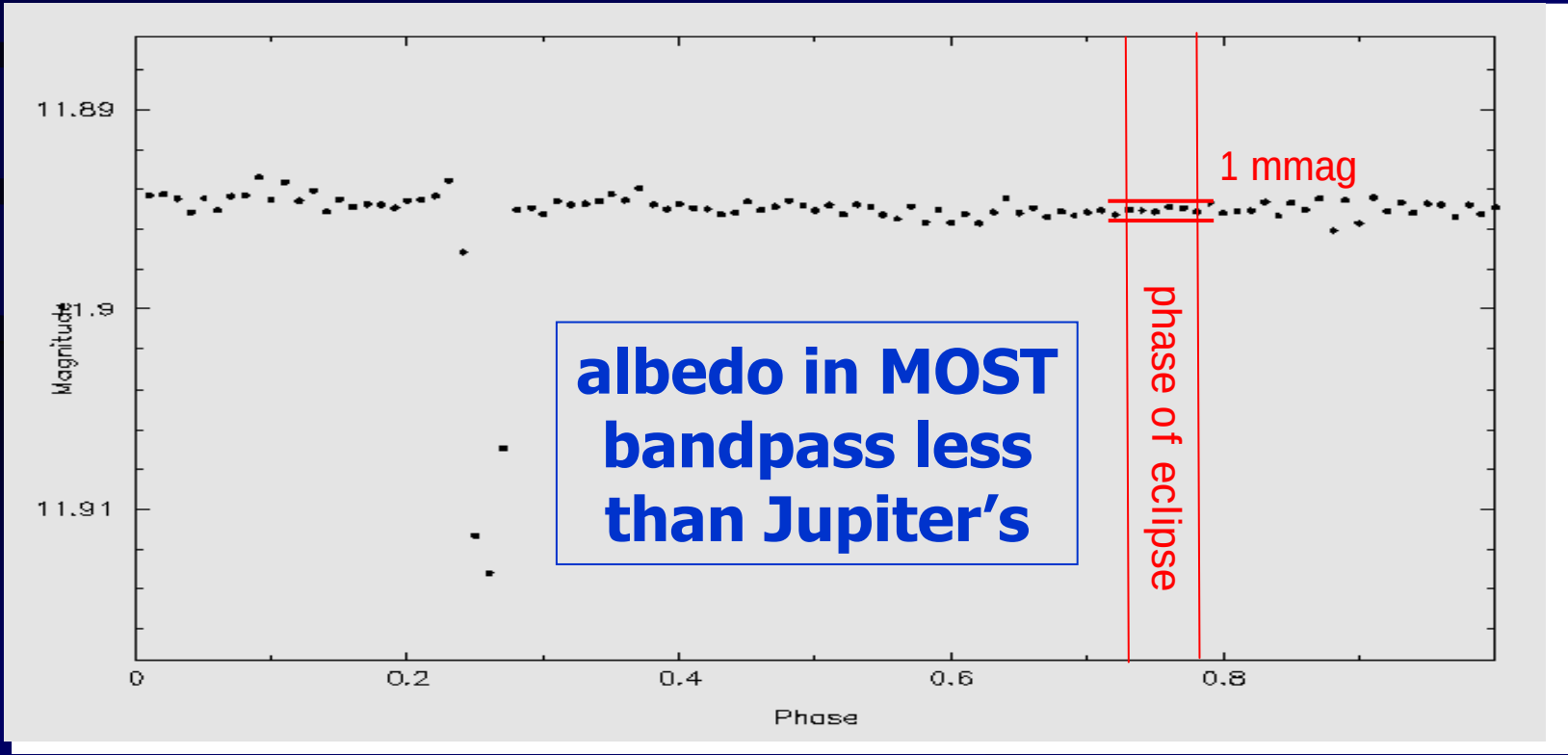

Conclusions

- We have built an instrument capable of measuring polarization to levels of ~10^{-6} in bright stars, around a factor of 100 better than previous stellar polarimeters.
- Results are stable and repeatable for normal stars without hot Jupiter planets.

- Present results suggest geometric albedo $p<0.2$ for Tau Boo and Upsilon And. 4x tighter limits or actual detection would be achieved with (i) an 8-m telescope; and (ii) low noise photodiode detectors.

- High sensitivity polarimetry may be valuable for a range of astronomical projects, eg. the ISM, debris discs, active stars and rapidly rotating stars.

- The technique may be valuable for future 8m or ELT instruments for planet detection.

Hot Jupiters are dark!

Problem

1) **Apart from a planetary surface, what other things might cause a polarisation signal to be detected when using a sensitive aperture polarimeter like planetpol?**

   List all that you can think of, whether in the planetary system or causes closer to the observatory.

High Resolution Polarimetry

- It is not clear that the stars in hot Jupiter systems are stable enough to detect planets though polarimetry at the 10^{-6} level.
- However when attempting to spatially resolve planets in large orbits polarimetry may be a powerful tool for suppressing the unpolarised stellar image.
- The challenge is to achieve a dynamic range of 10^{9} for planets in 3 to 5 AU orbits around nearby stars. This would permit observations of Jupiter-like planets of any age in reflected light. By contrast the emitted light can only be detected from very young planets much warmer than Jupiter.

- A polarimetric precision of only ~10^{-3}-10^{-4} may be necessary to suppress the stellar image profile to the level of photon noise. PLANETPOL has demonstrated that almost all single stars within 100 pc are unpolarised at this level.
- The challenge lies in the technology of Adaptive Optics.

Adaptive Optics Demo

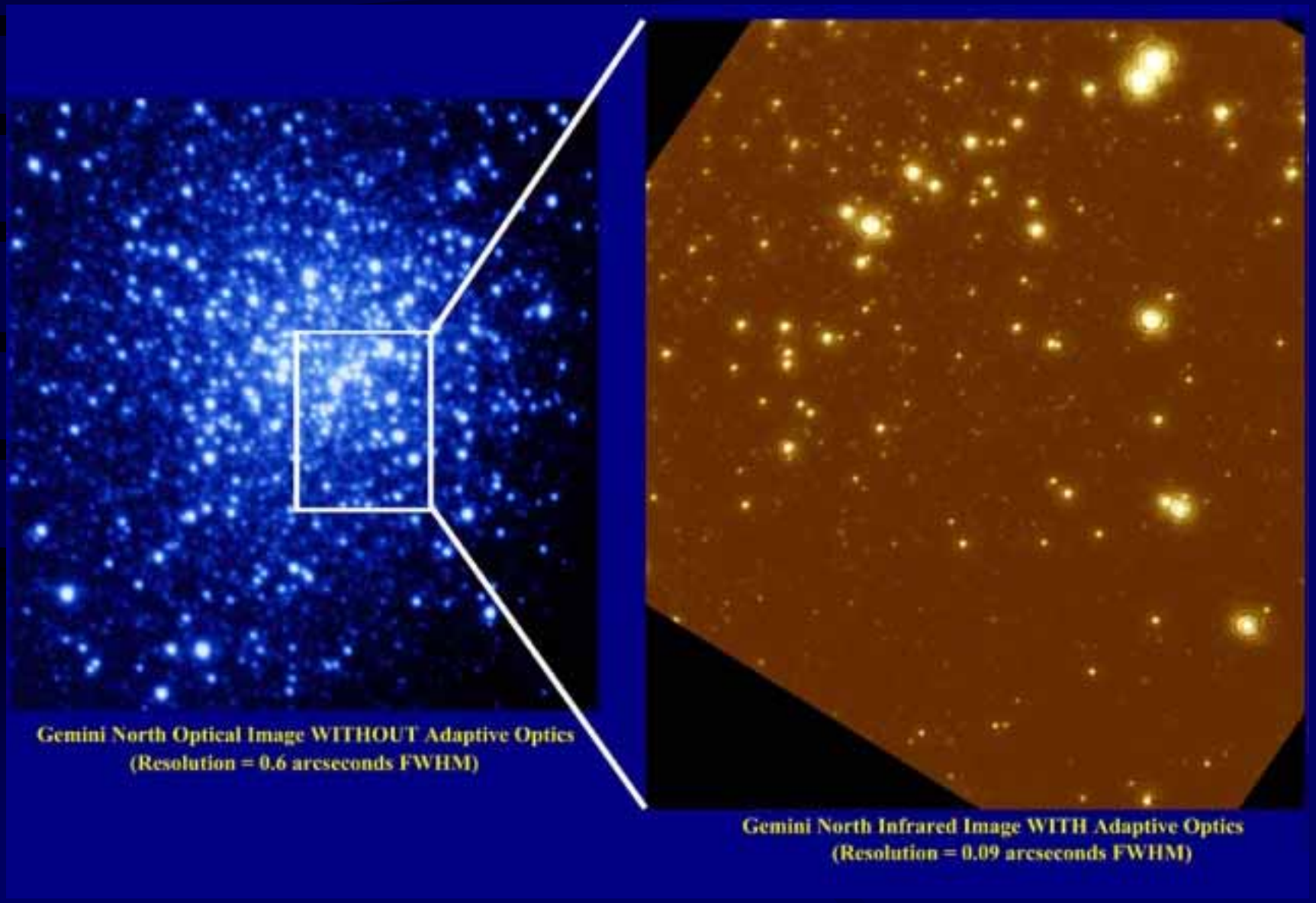

Gemini North Optical Image WITHOUT Adaptive Optics
(Resolution = 0.6 arcseconds FWHM)

Gemini North Infrared Image WITH Adaptive Optics
(Resolution = 0.09 arcseconds FWHM)

Principles of Adaptive Optics

- Normal images are blurred to a resolution of ~ 1 arcsec by the motion of turbulent air cells above the telescope aperture. These cells change the incoming wavefront from a smooth plane wave to a highly corrugated surface. A freeze frame image appears as many separate speckles focussed by different air cells within the aperture.

- Adaptive Optics (AO) technology smooths out the wavefront, thereby providing almost diffraction limited resolution:

  $\theta/\text{arcsec} = 206265 * (1.22\ \lambda/D)$.

  Key Elements of an AO system

  A bright reference star to provide light to characterise the wavefront.

  A high frequency (~1kHz) wavefront sensor and conjugating mirror.

- Simple AO systems with ~12 actuators can provide a sharp image, with resolution approaching the diffraction limit.
- But the diffraction limited core is surrounded by a seeing halo which is dominated by speckle noise.

Adaptive Optics Equations

- Strehl Ratio $S = I_{obs}/I_{unaberrated}$
- $S=\exp[-\sigma^2_{\varphi}]$ where σ^2_{φ} is the wavefront phase variance of the image, in units of radians^2.
- $\sigma^2_{\varphi} = C_j(D/r_0)^{5/3}$ in the Kolmogorov theory of atmospheric turbulence, where D is the telescope diameter, C_j is a coefficient dependent on the number, j, of Zernike modes corrected and r_0 is the Fried Coherence Length.
- $r_0 \alpha \lambda^{6/5}$. This is the size scale imposed by turbulent air cells at a range of altitudes in the atmosphere. It determines the size scale of the uncorrected seeing disc: $\theta = 1.22 \lambda / r_0$
- $C_j \approx 0.2944\ j^{-0.866}$ for large j.

Beckers J.M., 1993, Ann Rev A&A, 31, 13

Adaptive Optics Equations

Table 2 Modified Zernike polynomials and the mean square residual amplitude Δ_j (in rad^2) for Kolmogorov turbulence after removal of the first j Zernike polynomials[a]

Z_j	n	m	Expression	Description	Δ_j	Δ_j-Δ_{j-1}
Z_1	0	0	1	constant	1.030 S	
Z_2	1	1	$2r\cos\varphi$	tilt	0.582 S	0.448 S
Z_3	1	1	$2r\sin\varphi$	tilt	0.134 S	0.448 S
Z_4	2	1	$\sqrt{3}(2r^2-1)$	defocus	0.111 S	0.023 S
Z_5	2	2	$\sqrt{6}r^2\sin 2\varphi$	astigmatism	0.0880 S	0.023 S
Z_6	2	2	$\sqrt{6}r^2\cos 2\varphi$	astigmatism	0.0648 S	0.023 S
Z_7	3	1	$\sqrt{8}(3r^3-2r)\sin\varphi$	coma	0.0587 S	0.0062 S
Z_8	3	1	$\sqrt{8}(3r^3-2r)\cos\varphi$	coma	0.0525 S	0.0062 S
Z_9	3	3	$\sqrt{8}r^3\sin 3\varphi$	trifoil	0.0463 S	0.0062 S
Z_{10}	3	3	$\sqrt{8}r^3\cos 3\varphi$	trifoil	0.0401 S	0.0062 S
Z_{11}	4	0	$\sqrt{5}(6r^4-6r^2+1)$	spherical	0.0377 S	0.0024 S

[a] r = distance from center circle; φ = azimuth angle; $S = (D/r_0)^{5/3}$.

Methods of Increasing Dynamic Range beyond "simple" Adaptive Optics

- **a) Higher Strehl – limitations of no. of actuators, and no. of photons. Aim for S=0.9.**
- **b) Lyot coronograph – helps a bit but only a factor of 2 to 4 ?**
- **c) Nulling interferometry of AO corrected images – not clear if this can be done well enough from the ground.**
- **d) <u>Differential imaging</u> – subtract similar images taken in different filters or orthogonal polarisation states. This improves the dynamic range for polarised planets or planets with different colours than the star.**

Subaru/CIAO web page

Methods of Increasing Dynamic Range beyond "simple" Adaptive Optics

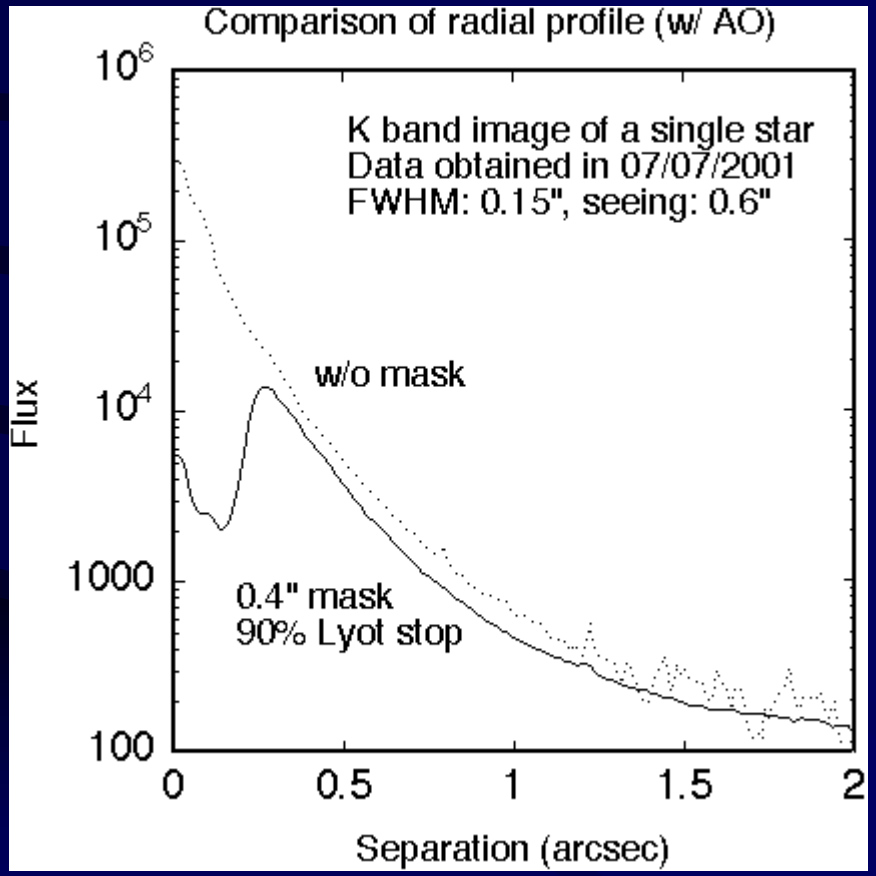

Examples of Diff

- IRAS 04016+2610 is a low mass Class I protostar in the Taurus-Auriga star formation region.
- The central light source is seen at λ>2 um and has a polarisation of ~4%.
- It illuminates a reflection nebula which is highly polarised (up to 80%).

- The polarised flux image (obtained with the dual beam polarimeter IRPOL-2 at UKIRT) suppresses the central source, revealing what appear to be 2 bipolar cavities where light can easily escape the system.

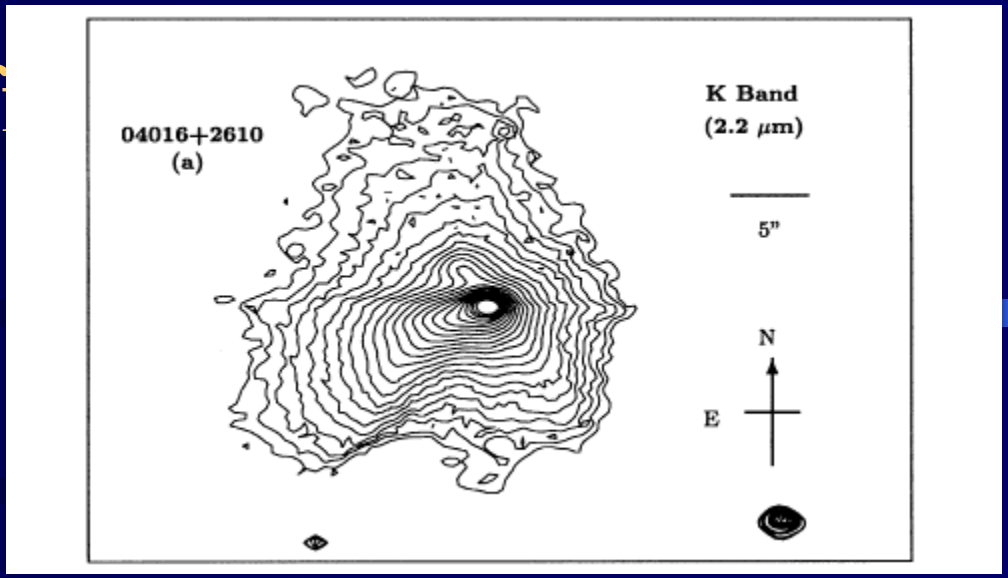

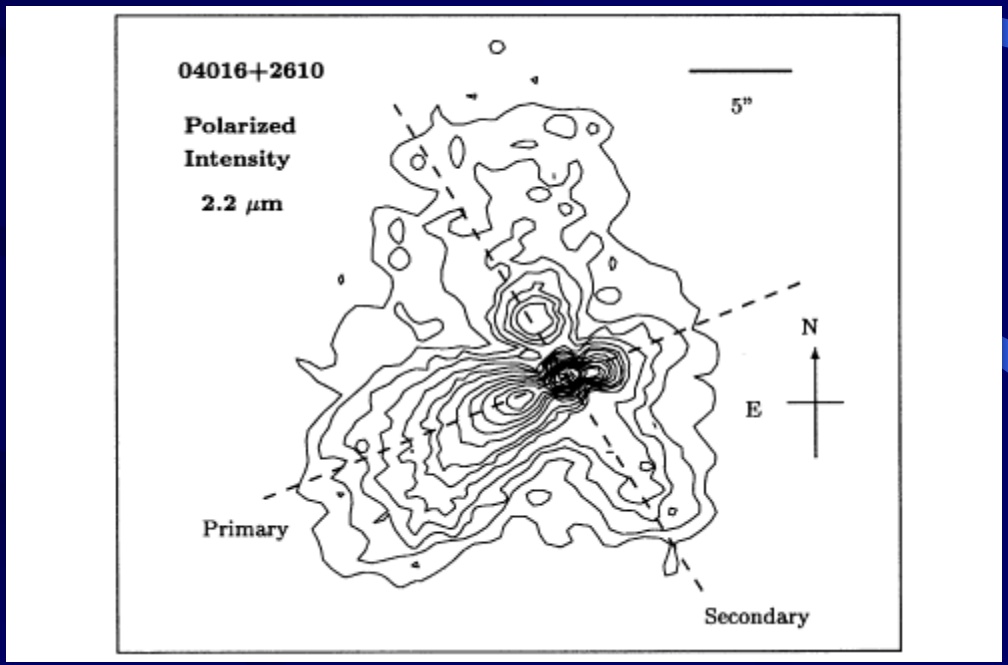

Differential Imaging (2)

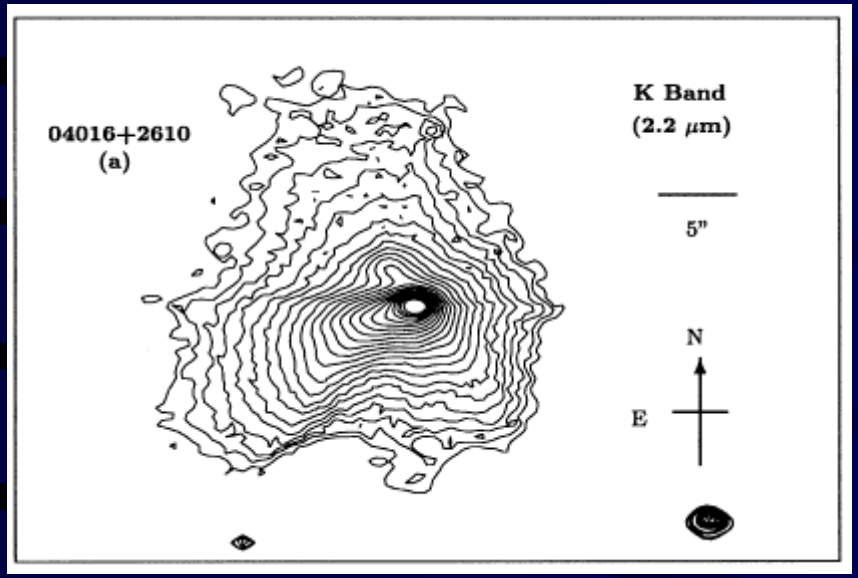

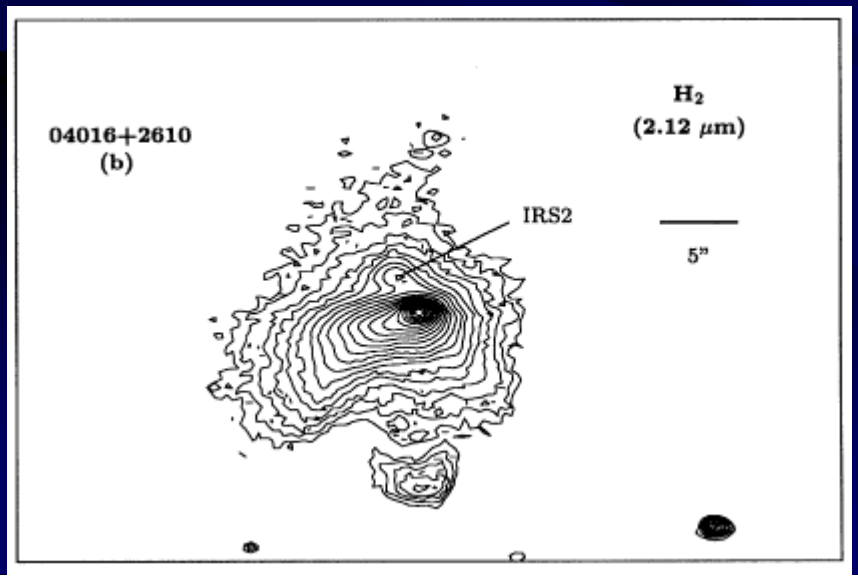

Imaging in narrow band filters ($\Delta\lambda/\lambda=0.01$) is commonly used to observe emission line nebulae. Difference imaging of 04016+2610 in H_2 – K (2.0 to 2.4 um) reveals an H_2 emitting bow shock and shows the reddening gradient caused by extinction differences in the central region.

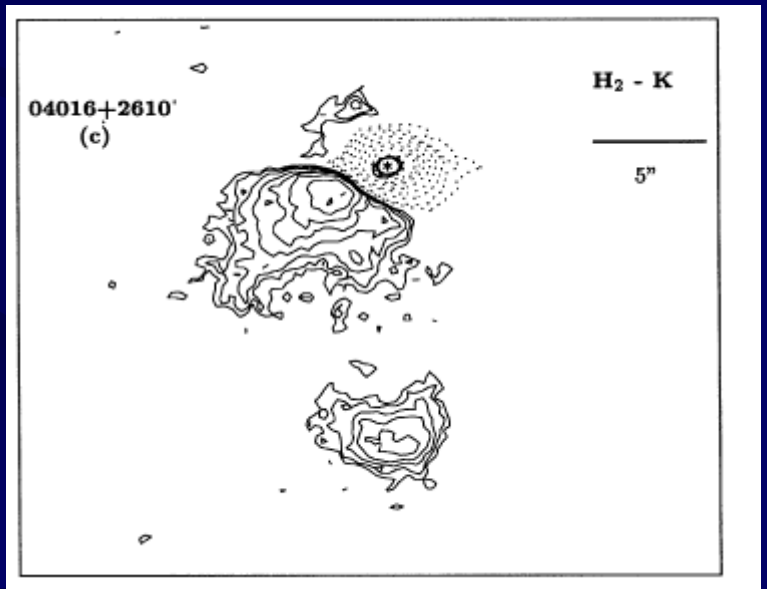

Differential Imaging (3)

- Differential imaging with AO systems works best when the 2 images are obtained simultaneously, so that the random speckle noise pattern is very similar in both images.
- Subtraction of 2 AO-corrected images gives attenuation

  $A_2 = 2\sigma^2_\varphi \, \Delta\lambda/\lambda$ where σ^2_φ is the wavefront phase variance of each image. This is due to the different Strehl ratios in the different filters.

- Double difference imaging with 3 narrow band filters can remove nearly all the speckle noise from an AO image (Marois et al.2000, PASP 112,91) by correcting for the differences in Strehl ratio.
- In theory the attenuation factor using 3 AO-corrected images is $A_3 \sim A^2_2$.

- Referred to as Simultaneous Differential Imaging (SDI) by the NACO-SDI group, see www.mpia.de/NACO/SDI-index.html.

Differential Imaging (3)

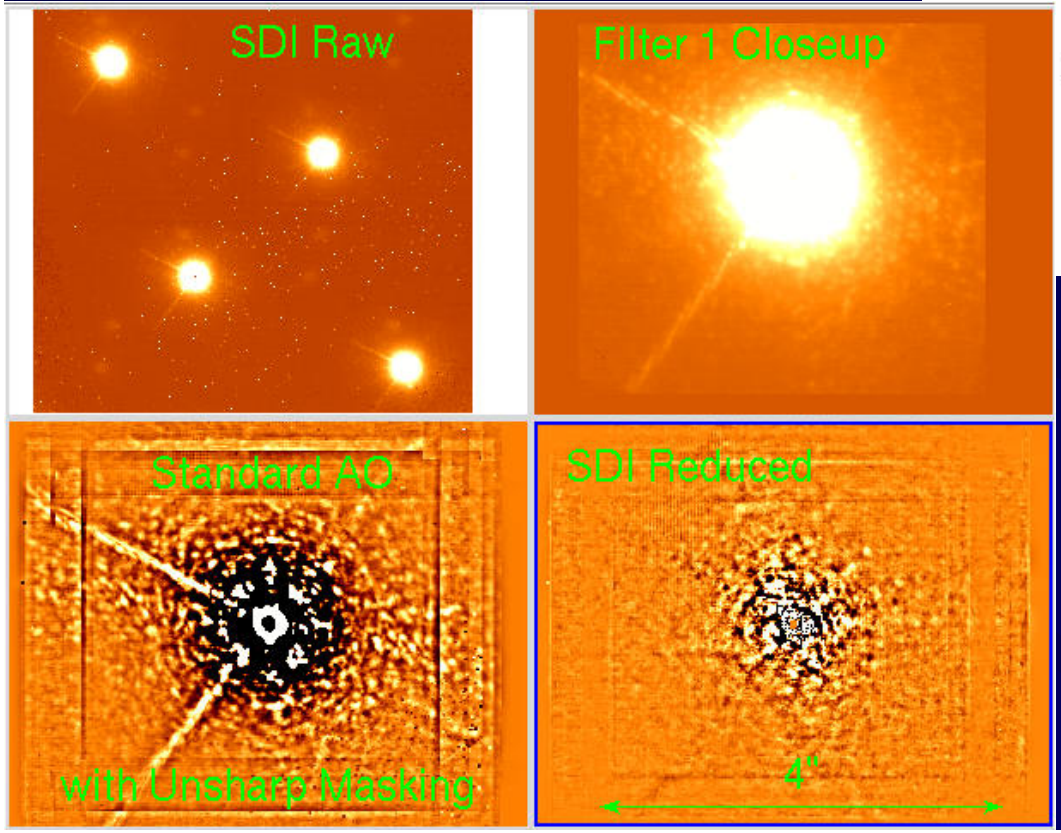

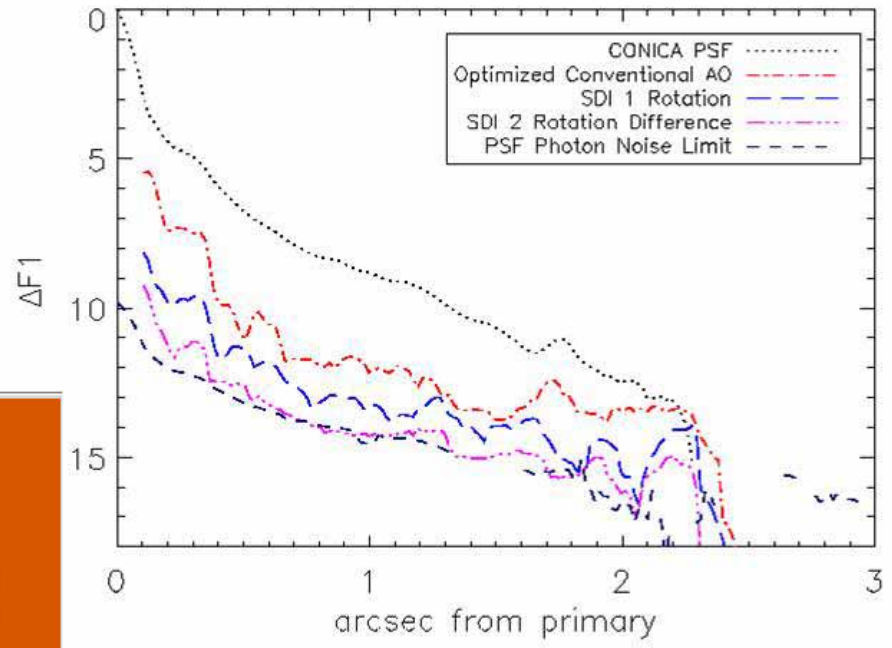

Strengths and weaknesses of these techniques

- The SDI method is limited to planets with strong and narrow spectral features in the near infrared, eg. CH_4. Hence the method provides detections only at specific wavelengths.
- Absorption features may occur in old planets observed in reflected light as well as warm young planets.

- Polarimetry may provide a wider wavelength coverage than SDI but it cannot detect planets with low reflectivity. It is not useful for warm young planets which are bright and relatively easy to see in emitted light.

Problems

- 2a) If only 100 actuators are available and they perfectly correct the first 100 Zernike modes, what is the biggest telescope that can achieve S=0.9 at 1.6 microns in good seeing conditions, such that r_0=20cm at 0.55 um.

- 2b) If only 100 actuators are available, but an 8-m aperture is desired to collect many photons from the planet, what is the minimum wavelength at which S=0.9 can be achieved?

Equations

- Strehl Ratio $S = I_{obs}/I_{unaberrated}$
- $S=\exp[-\sigma^2_{\varphi}]$ where σ^2_{φ} is the wavefront phase variance of the image.
- $\sigma^2_{\varphi} = C(D/r_0)^{5/3}$ where D is the telescope diameter and r_0 is the Fried Coherence Length.
- $r_0 \alpha \lambda^{6/5}$
- $C_j \approx 0.2944\ j^{-0.866}$ for large j.

Modelling Polarisation Data

- The magnitude and shape of a planetary polarisation signal depends on orbital inclination, orbital radius, the composition and size of the scattering particles and the wavelength.
- Hence with good data we determine the Inclination, I, (and then mass if m.sin(i) is known), albedo in 3 colours, the nature of the scattering particles (Rayleigh or dust particles or drops of rain or ammonia…), planet radius and approximate temperature.

Published approach no.1
Seager, Whitney and Sasselov,
2000, Ap. J. 540, 504.

They used Monte Carlo modelling of Dust grains with a full atmospheric model. Dozens of molecular and atomic species were included.

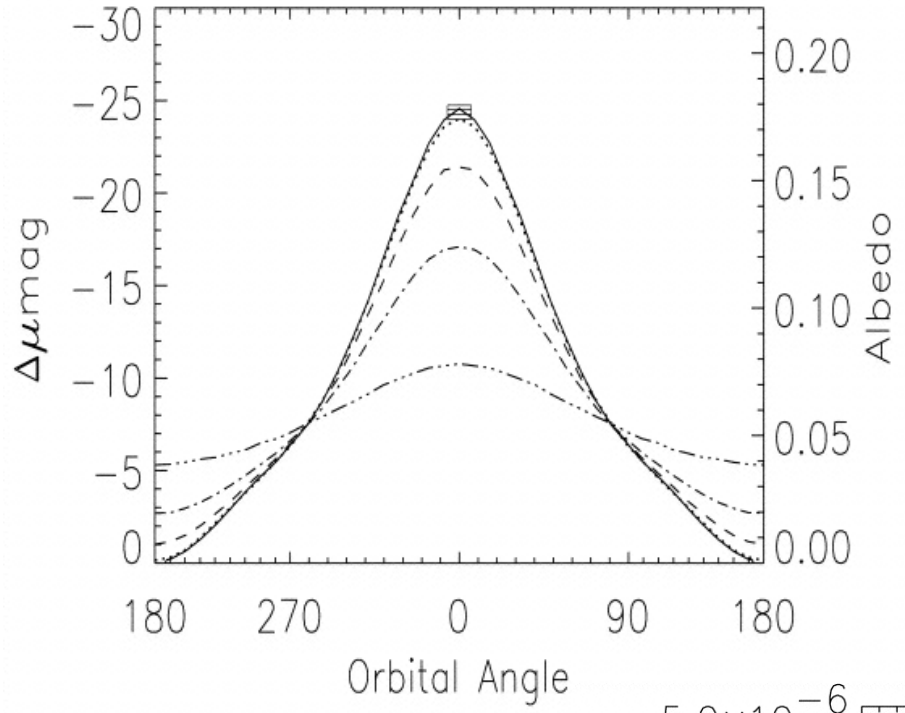
−30
−25
−20
−15
−10
−5
0
Δμmag
0.20
0.15
0.10
0.05
0.00
Albedo
180
270
0
90
180
Orbital Angle

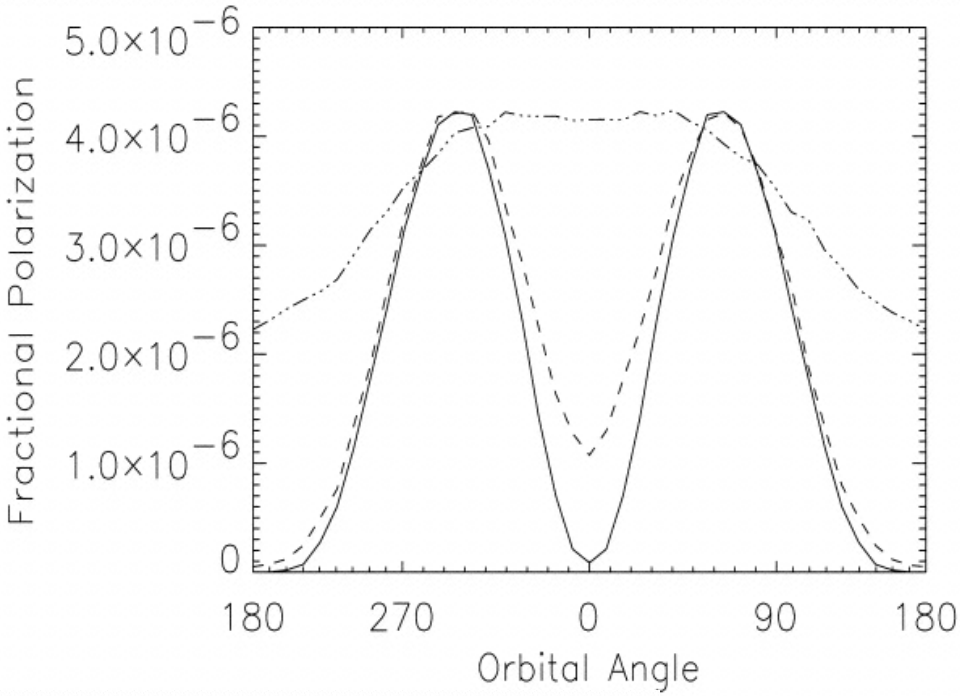
5.0×10−6
4.0×10−6
3.0×10−6
2.0×10−6
1.0×10−6
0
Fractional Polarization
180
270
0
90
180
Orbital Angle

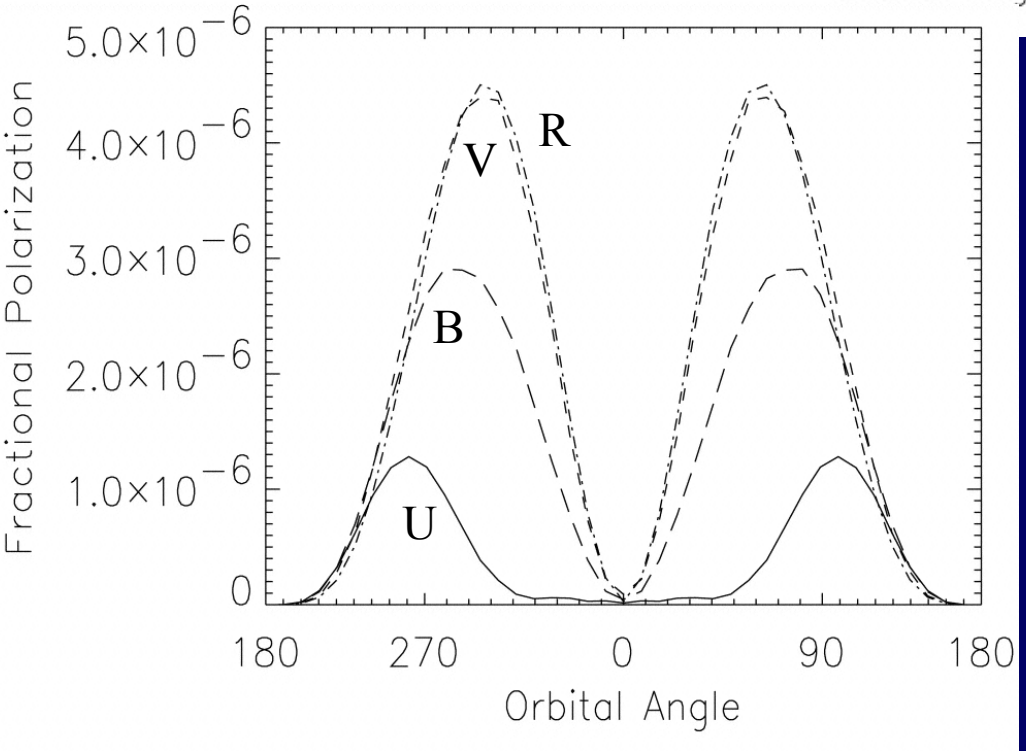
5.0×10−6
4.0×10−6
3.0×10−6
2.0×10−6
1.0×10−6
0
Fractional Polarization
V
R
B
U
180
270
0
90
180
Orbital Angle

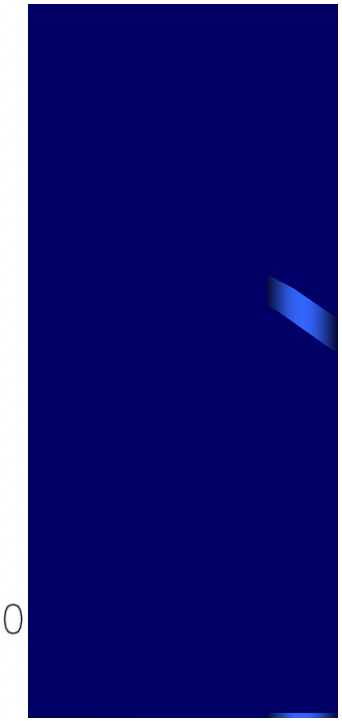

Effect of Grain Size

- Small grains scatter light in a Rayleigh-like way.
- The phase function is almost isotropic.
- Large grains (size parameter $x=2\pi r/\lambda > 1$) have a highly forward throwing phase function, and sometimes there is a back-scattering peak also, though this is weak in real, imperfectly spherical grains.
- Large grains are bad news for optical and near IR planet detection, since most of the light is forward scattered deep into the atmosphere and never returns.

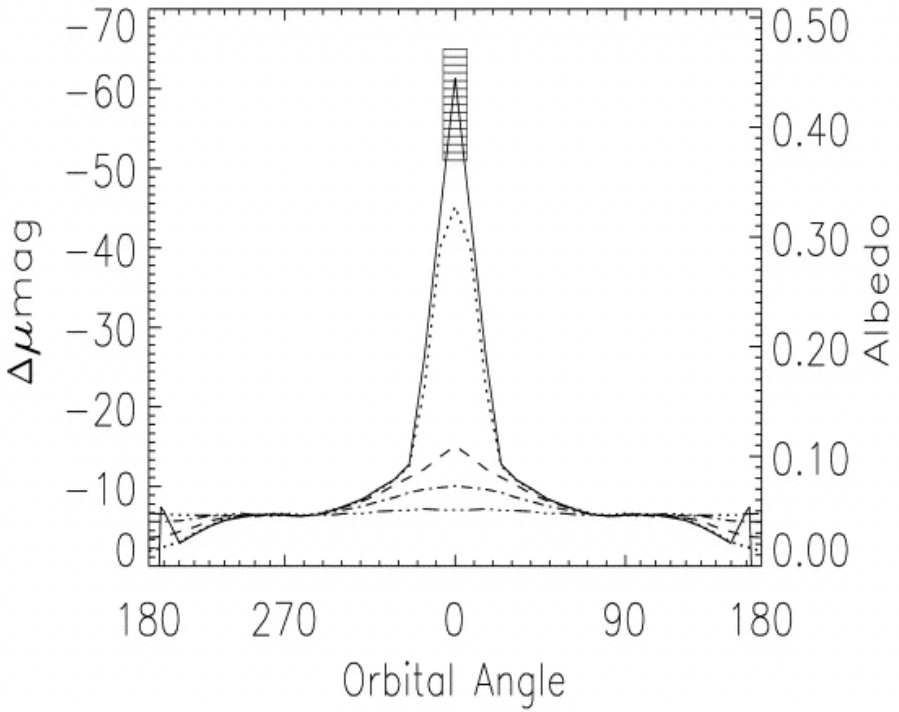

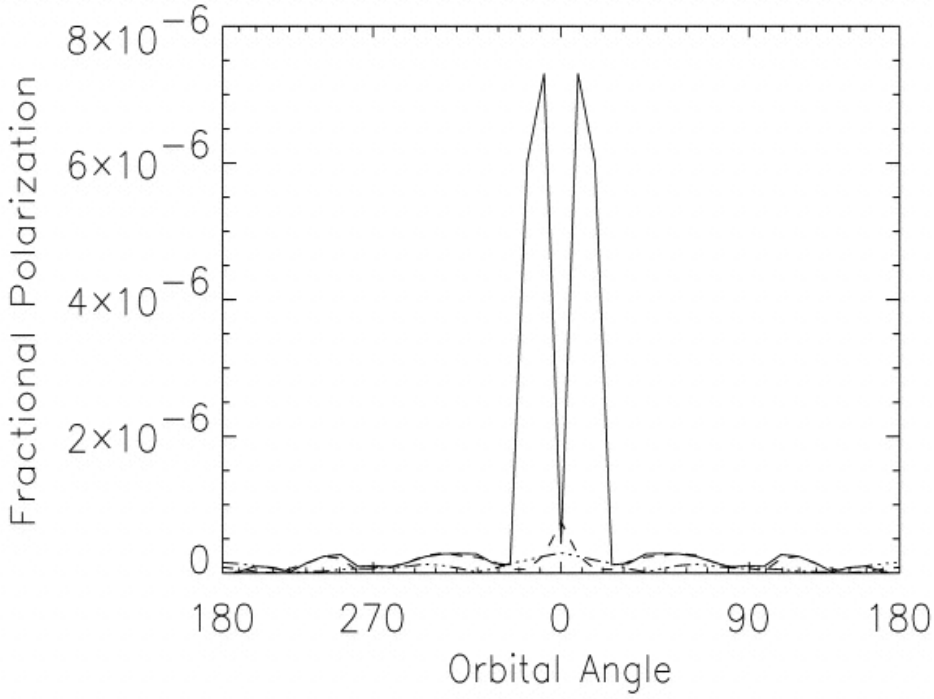

Albedo Definitions

- The geometric albedo, *p*, is the ratio of the reflected flux from a planet at full moon phase to that reflected by a Lambert disc of the same size.
- A Lambert disc is a perfectly reflecting matt surface (isotropic phase function).
- *p* is the most useful quantity for observers.
- The Bond albedo, *A*, is the ratio of the light reflected by the planets in all directions to that received from the star.
- *A* controls the planet's energy budget.
- $A = pq$, where q is the integral of the phase function from 0 to π.
- A Lambert Sphere has $A = 1$, $p = 2/3$, $q=3/2$.

Monte Carlo simulations

- The term Monte Carlo refers to calculations involving random (stochastic) processes.
- The emission, scattering and absorption of photons is a classic example of this.
- To simulate the polarisation of a planet we generate millions of unpolarised photon packets (I,Q,U,V)=(1,0,0,0) at random locations on the stellar surface and allow them to land at random locations on the hemisphere of the planet facing the star.
- The photons then within the atmosphere, being scattered in random directions sampled from the phase function until they are absorbed or reflected back into space.
- Photons which escape are binned by outgoing direction and add their Stokes vector to the calculation for their appropriate bin.

Calculation of a Stokes vector after scattering

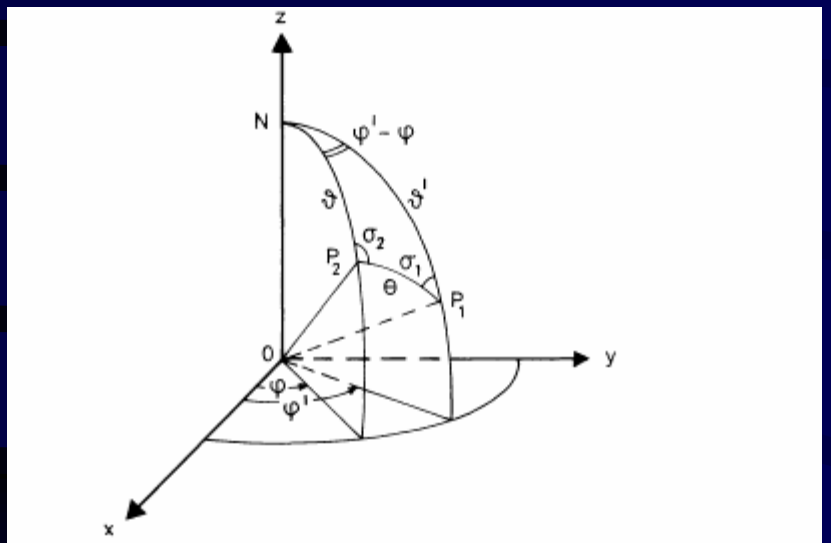

Fig. 2. Scattering by a local volume-element at O. Points N, P_1 and P_2 are on a unit sphere. The direction of the incident light is OP_1. The scattered light is in the direction OP_2. Here $0 < \varphi' - \varphi < \pi$

The calculation is simplified by doing it in the plane defined by the incident ray and the scattered ray, which is called the scattering plane.

Scattering

$$\begin{pmatrix} I \\ Q \\ U \\ V \end{pmatrix}_{scat} = \mathbf{L}(\pi - \sigma_2)\ \mathbf{Z}\ \mathbf{L}(-\sigma_1) \begin{pmatrix} I \\ Q \\ U \\ V \end{pmatrix}_{inc}$$

where the Stokes matrix $\mathbf{Z} = \begin{pmatrix} Z_{11} & Z_{12} & Z_{13} & Z_{14} \\ Z_{21} & Z_{22} & Z_{23} & Z_{24} \\ Z_{31} & Z_{32} & Z_{33} & Z_{34} \\ Z_{41} & Z_{42} & Z_{43} & Z_{44} \end{pmatrix}$

but Z_{41}, Z_{42} are zero for spheres:

$$\mathbf{Z} = \begin{pmatrix} Z_{11} & Z_{12} & 0 & 0 \\ Z_{12} & Z_{11} & 0 & 0 \\ 0 & 0 & Z_{33} & Z_{34} \\ 0 & 0 & -Z_{34} & Z_{33} \end{pmatrix}$$

- **Hovenier & van der Mee 1983, A&A 128, 1.**

Sampling a Probability Distribution

- **For simple equations we can derive the Cumulative Distribution Function (CDF) from the Probability Density Function (PDF) and invert the function. Eg.**

PDF: P(photon penetrates τ) = exp(-τ) for each photon.

CDF = Integral of exp(-τ) = 1- exp(-τ) .

So R=1- exp(-τ)

τ = -ln(1-R).

Eg. an unusually determined photon with R=0.9 penetrates an optical depth τ = 2.30.

Rejection Sampling

- **It is often impossible to invert more complicated or transcendental equations so Rejection Sampling is used.**

- **Eg. to sample the scattering deflection angle (DEF) from a complicated non-isotropic function F(DEF):**

```
10    Generate HARVEST_1                (HARVEST is the Fortran90
      DEF=PI*HARVEST_1                  random number generator)
      P(DEF)=F(DEF)/MAX(F(DEF))
      Generate HARVEST_2
      IF HARVEST_2 > P(DEF) THEN
      GOTO 10
      ELSE
      ACCEPT ANGLE DEF
      END IF
```

HL Tau – Polarised Flux

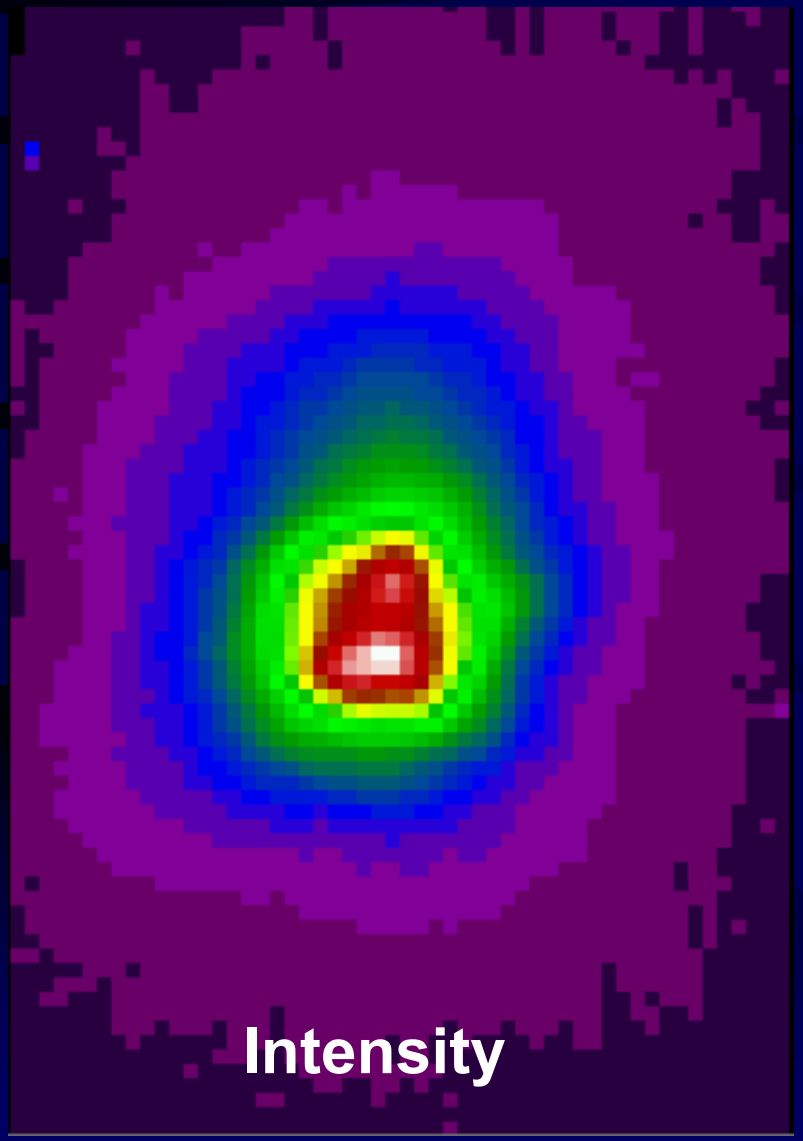

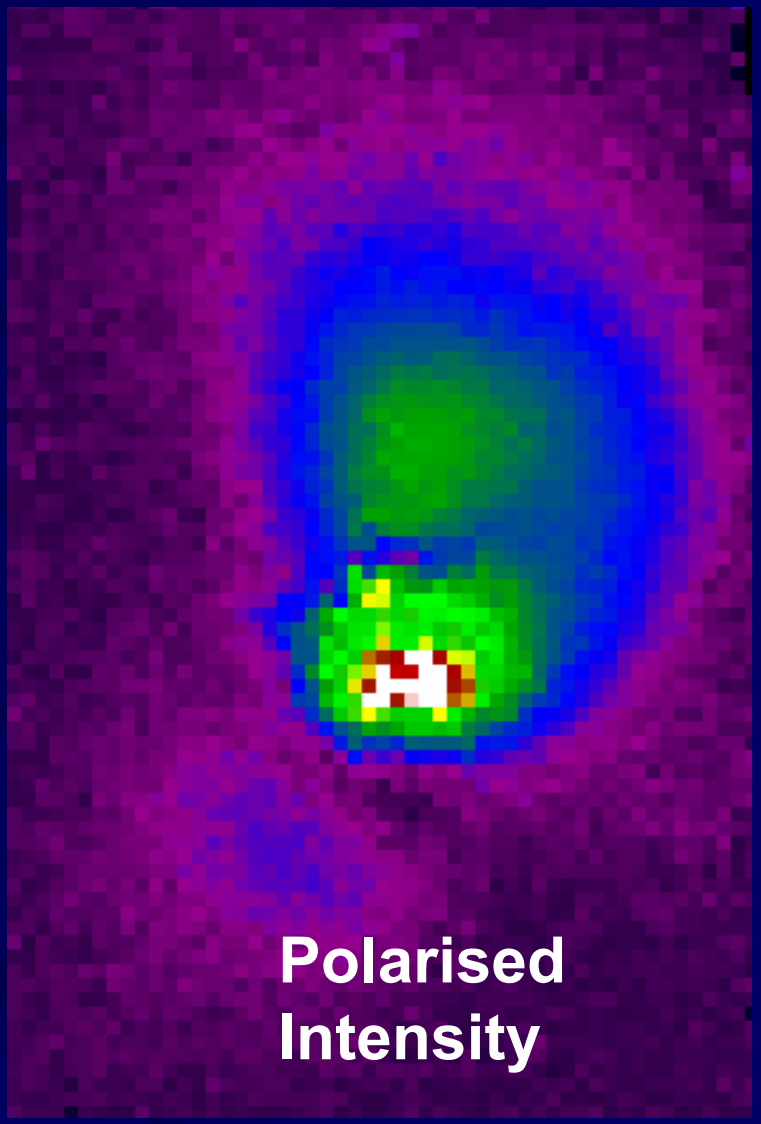

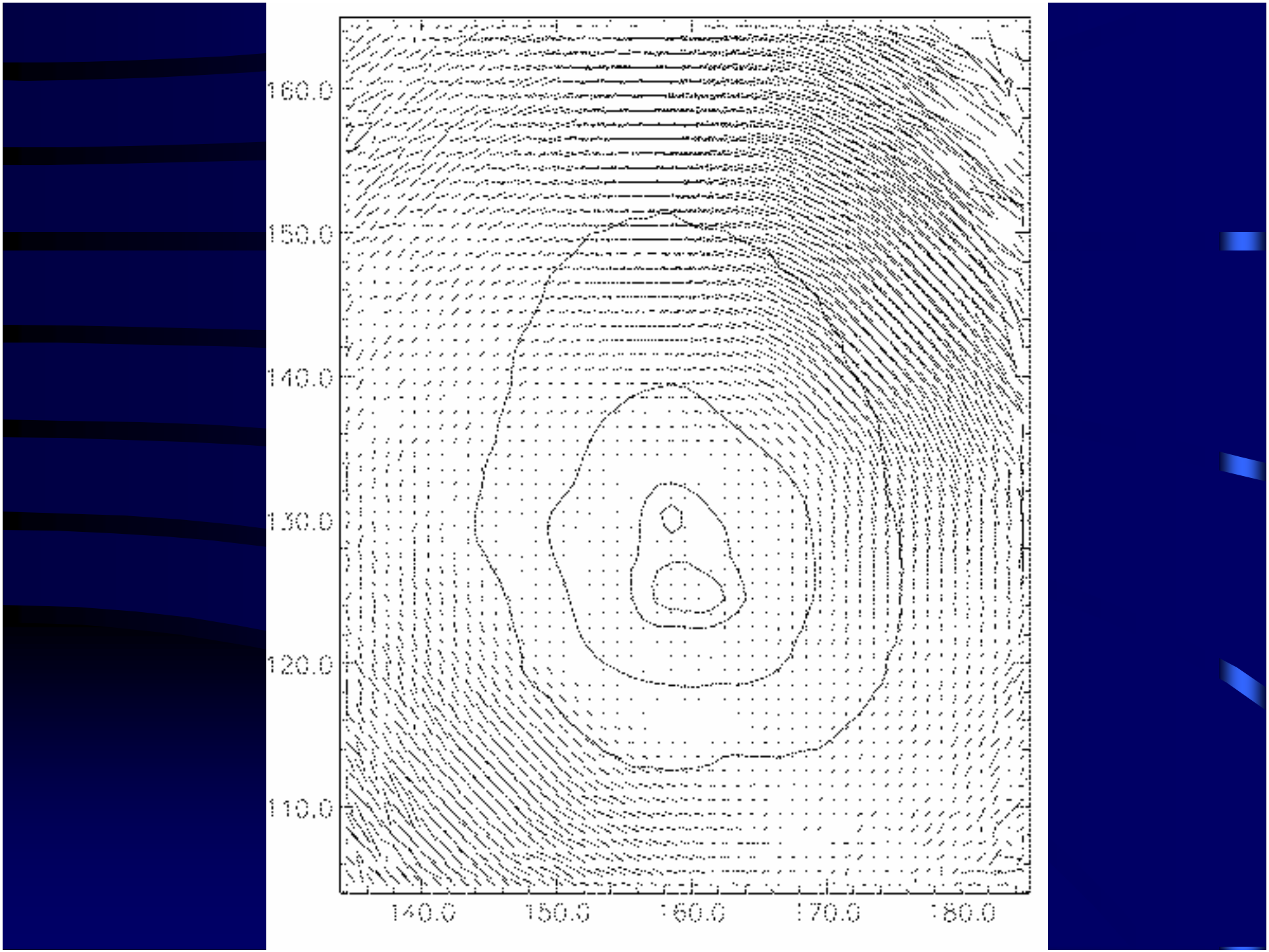
160.0
150.0
140.0
130.0
120.0
110.0
140.0
150.0
160.0
170.0
180.0

Cartoon of the model

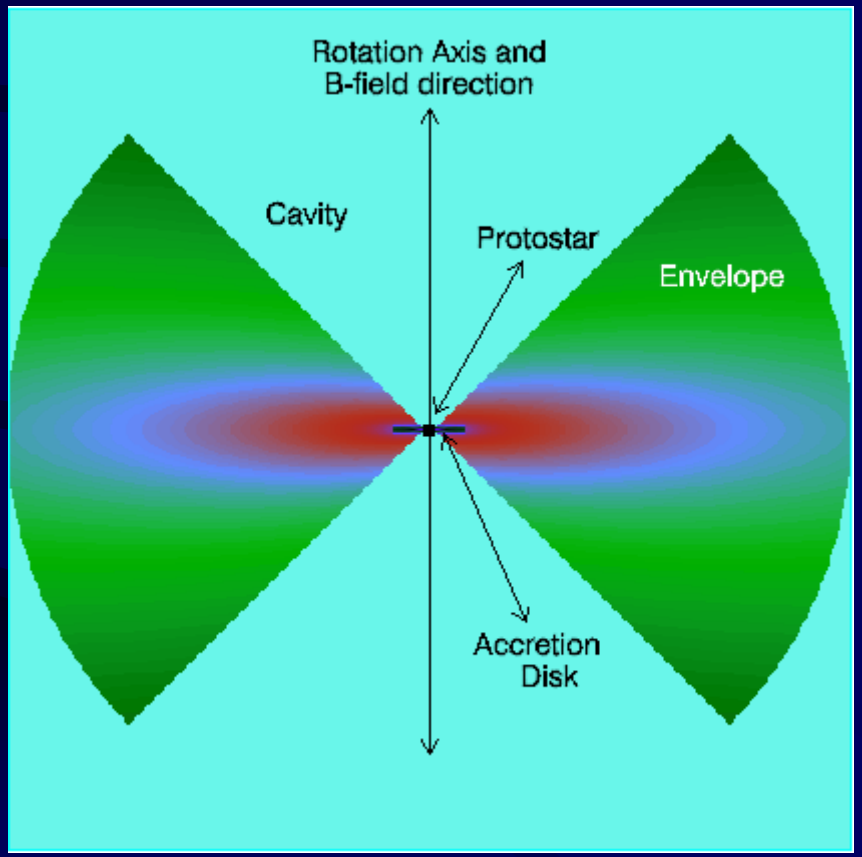

Simulation Results

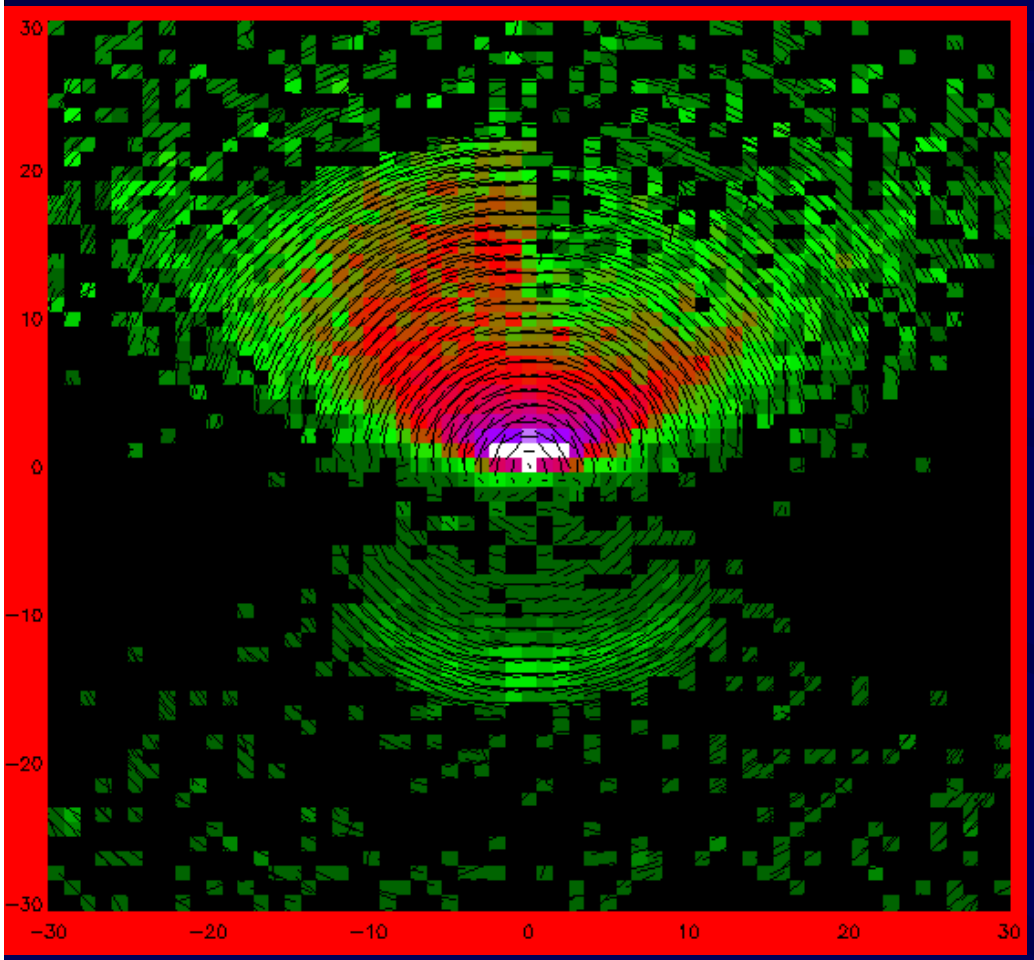

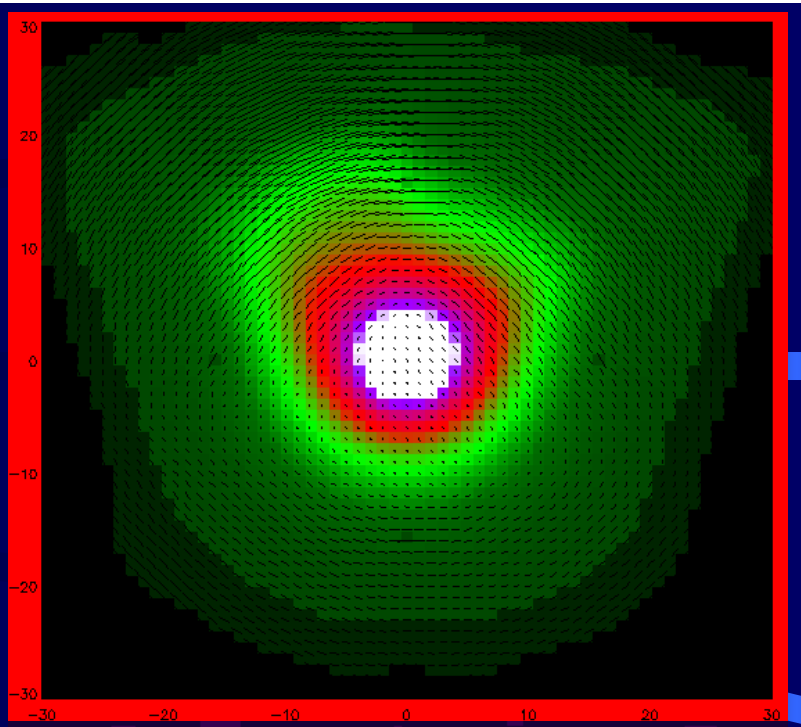

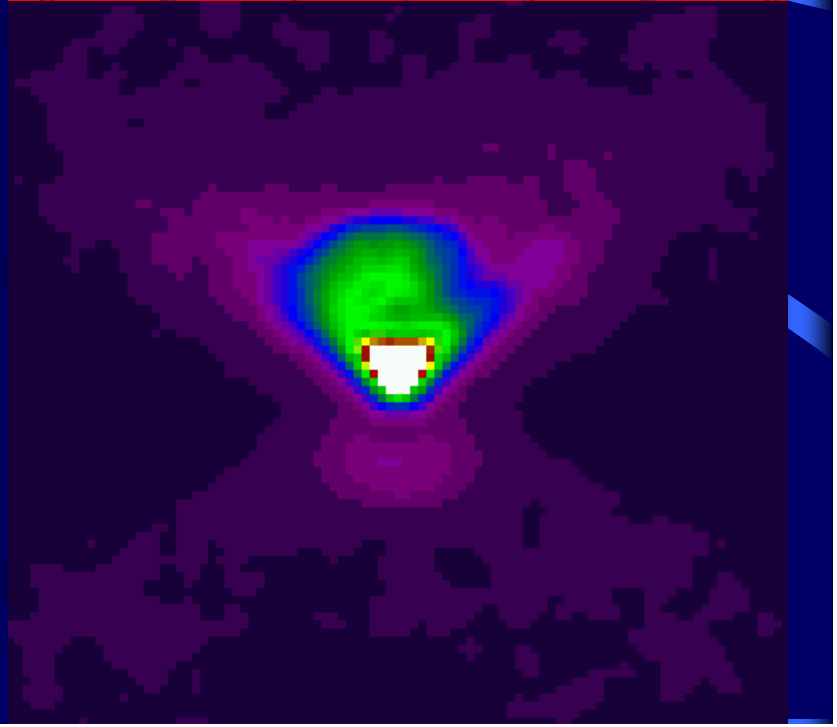

The Adding Doubling Method

- An alternative to the Monte Carlo method, suitable for radiative transfer in atmospheres which can be described by a limited number of different plane parallel homogeneous layers.
- Consider just 2 layers, which may be identical or different.

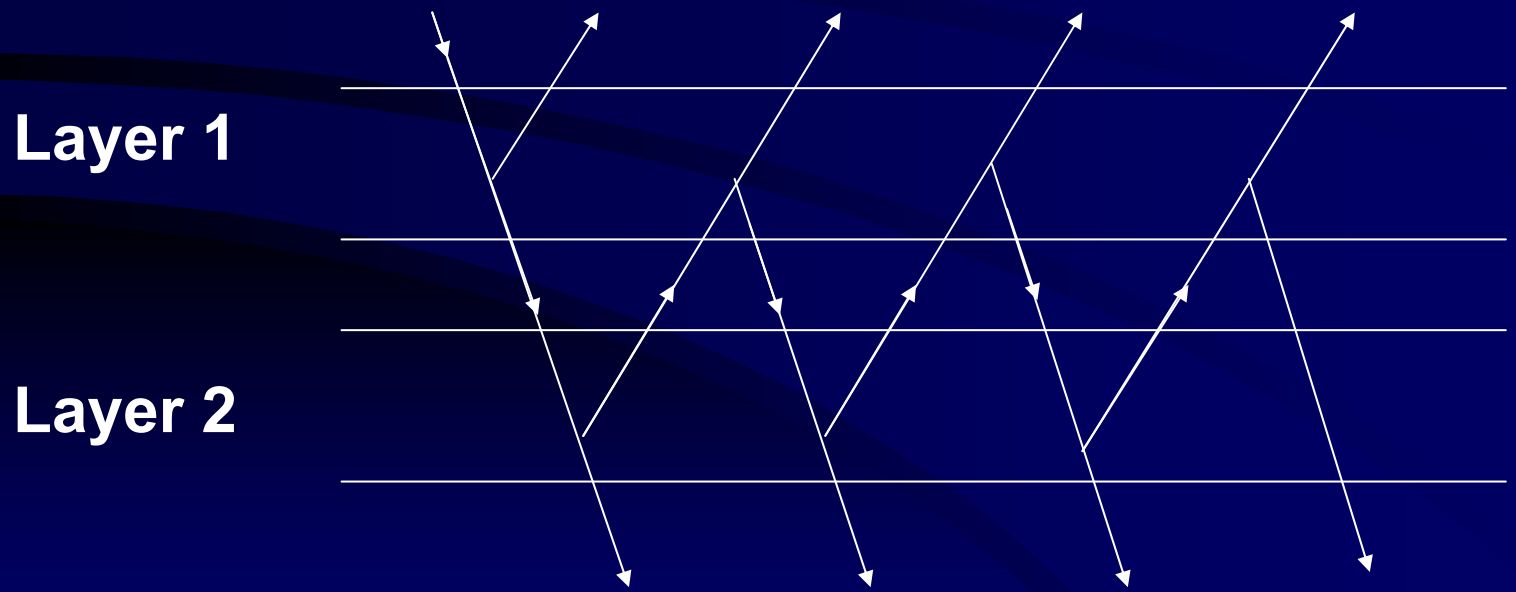

The Adding Doubling Method

- $I_{ref}(\mu) = \int_0 R(\mu, \mu_0)\, I_{in}(\mu_0)\, 2\mu_0\, d\mu_0$ where μ is cos(angle to vertical)
- Represent as $I_{ref} = RI_{in}$
- Then $R(2\ layers) = R_1 + T_1R_2T_1 + T_1R_2R_1R_2T_1 + \ldots..$
- $T\ (2\ layers) = T_1T_2 + T_1R_2R_1T_2 + T_1R_2R_1R_2R_1T_2 + \ldots..$

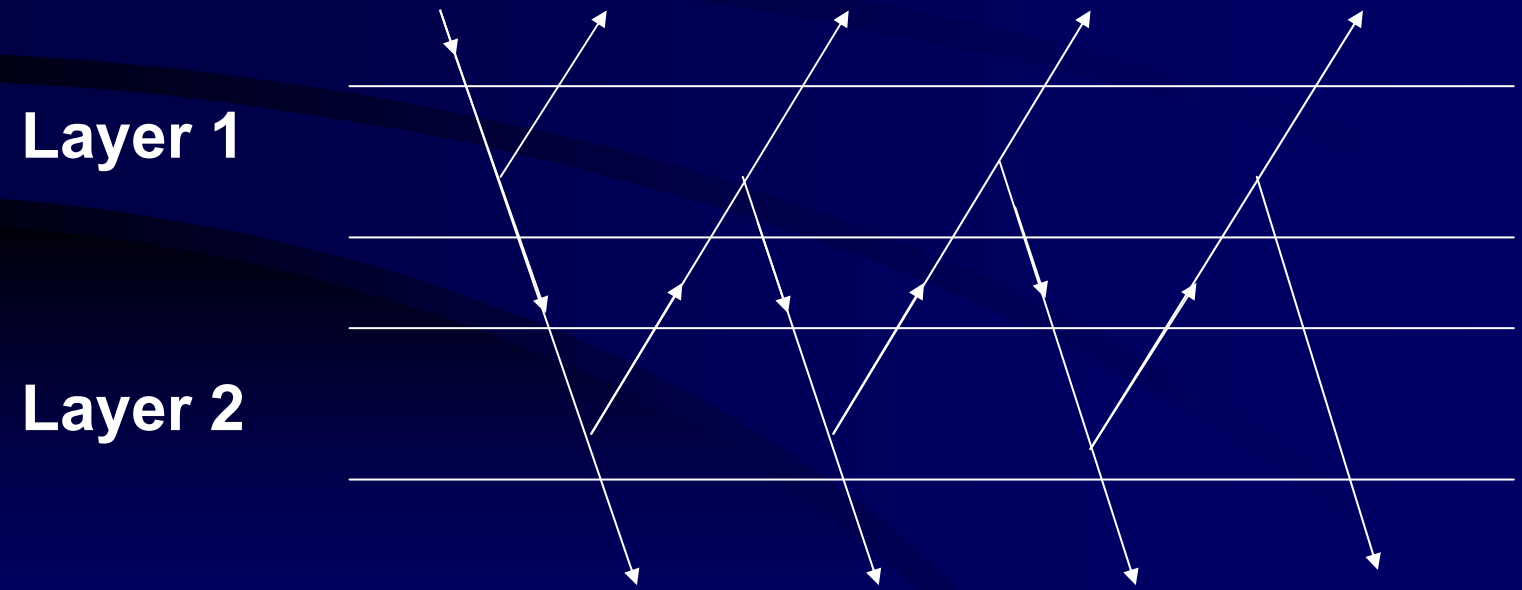

The Adding Doubling Method (2)

- Optically thin layers can be computed with a sum of a fairly small number of terms. The terms in **I** converge in a geometric series after a while, but terms in Q and U do not quite follow a geometric series.
- Optically thick layers can be built up be adding 2 identical layers ($R_1 = R_2$, $T_1 = T_2$), then repeating the process several times – this is the Doubling Method.
- A full model atmosphere may then be built up be adding layers of different composition – the Adding Method.
- This method is mathematically and computationally pretty complicated but a lot of work has been done with it.

Adding Doubling Method (3)

- Stam, Hovenier & Waters (2004, A&A 428, 663).
- Models assume a Jupiter-like Pressure-Temperature profile and consist of 38 layers across the range 10^{-4} bar < P < 5.6 bar.
- The main molecular absorber at 0.4 um < λ < 1.0 um is CH_4. A 0.18% mixing fraction is assumed.

- Model 1 – no particles, just molecules.
- Model 2 – 'low clouds' added.
- Model 3 – low clouds' and 'high altitude haze' added.

Calculation for orbital phase angle = 96^o

Flux and Polarisation averaged over 0.65 to 0.95 um wavelength range.

Adding Doubling Method (3)

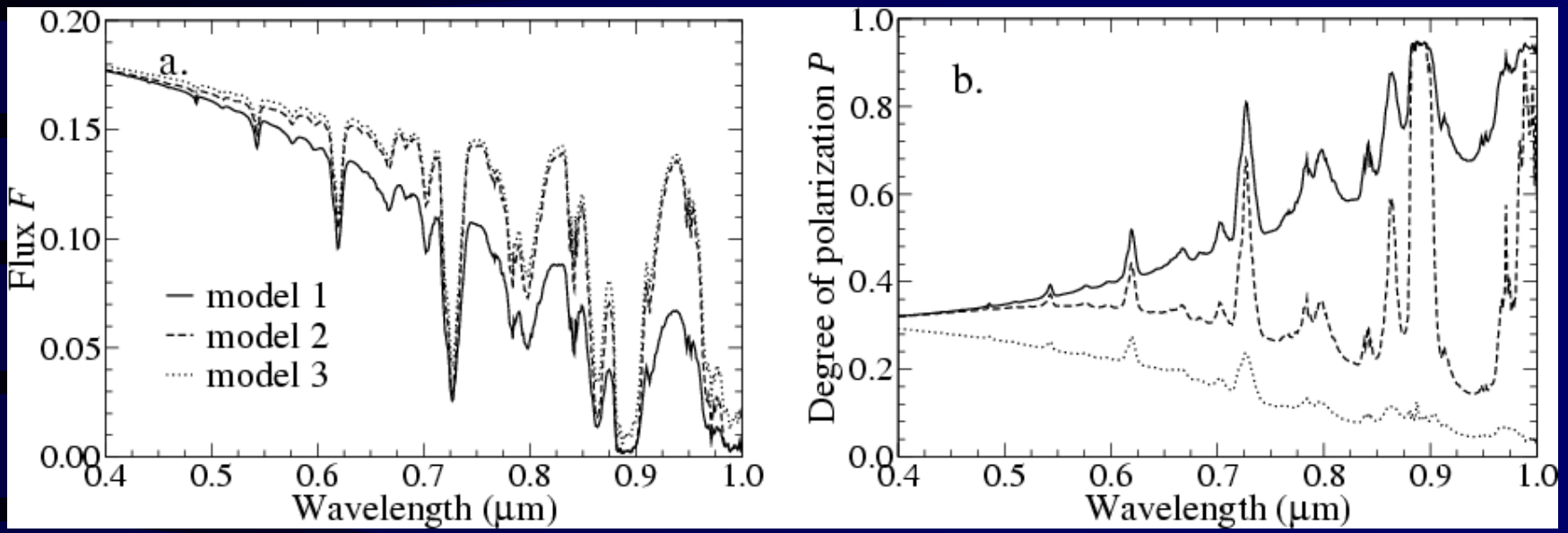

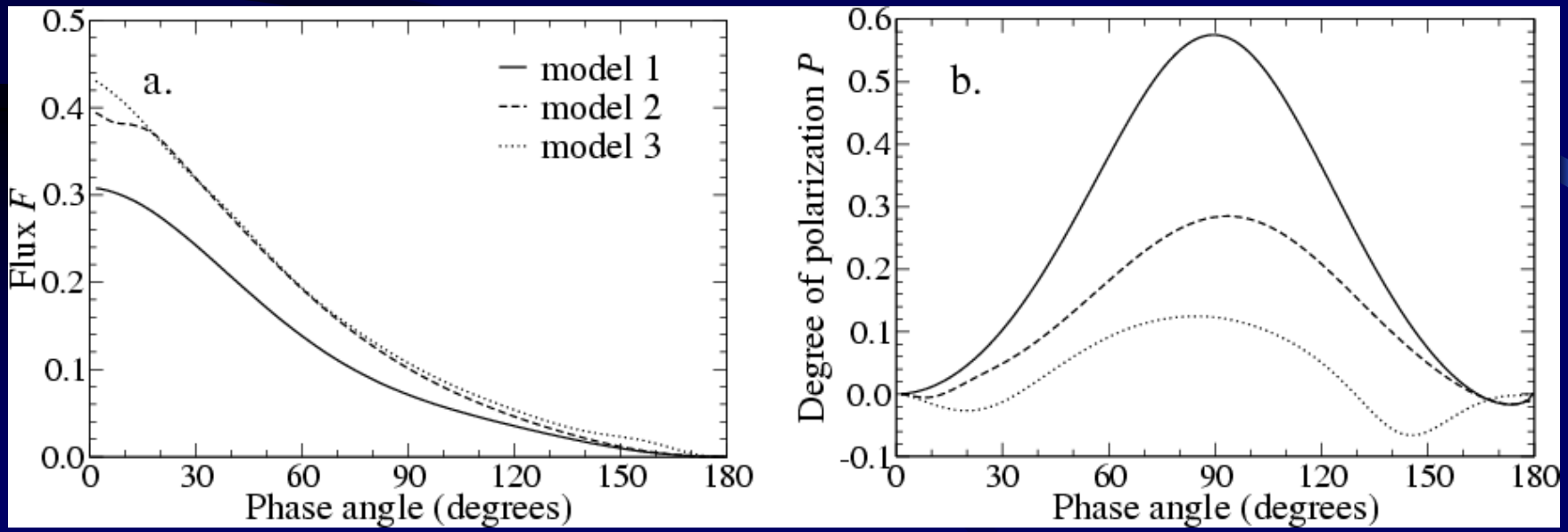

Problem

3) Hot Jupiter planets are most likely surrounded by a very large halo of free electrons and protons, due to the intensive ionisation of the planetary atmosphere. Make a rough estimate of the ratio of the polarisation signal from a hot Jupiter due to Thompson scattering off the cometary halo to that produced by the planet itself.

Assume: planetary radius is 1.2 R_{Jup} ;halo size scale = 10 R_{Jup} ; planet and halo are located at distance r~20 R_{Jup} from the star; halo column density is 10^{22} – 10^{23} electrons/m^2 (model by Jean Schneider).

Is the halo signal likely to seriously contaminate the planetary Signal?

Data: $\sigma_{th} = 6.65 \times 10^{-29}$ m^2

$R_{Jup} = 7 \times 10^7$ m.

Planetary Mass Objects in Star Formation Regions

- Very young brown dwarfs have been directly imaged in star formation regions with masses apparently similar to those of massive planets.
- They have surface temperatures similar to hot Jupiters and cool M- and L-type stars (1500 – 2500K).
- They are physically larger than planets like Jupiter or field brown dwarfs since they are still contracting towards a radius of $1R_{Jup}$,which is determined largely by the pressure of the degenerate core.
- Owing to their large size they have a low surface gravity, which is used to distinguish them from field brown dwarfs through spectroscopy.

The Trapezium Cluster in Orion
(UKIRT IJH image)

Planetary Mass Objects in Star Formation Regions

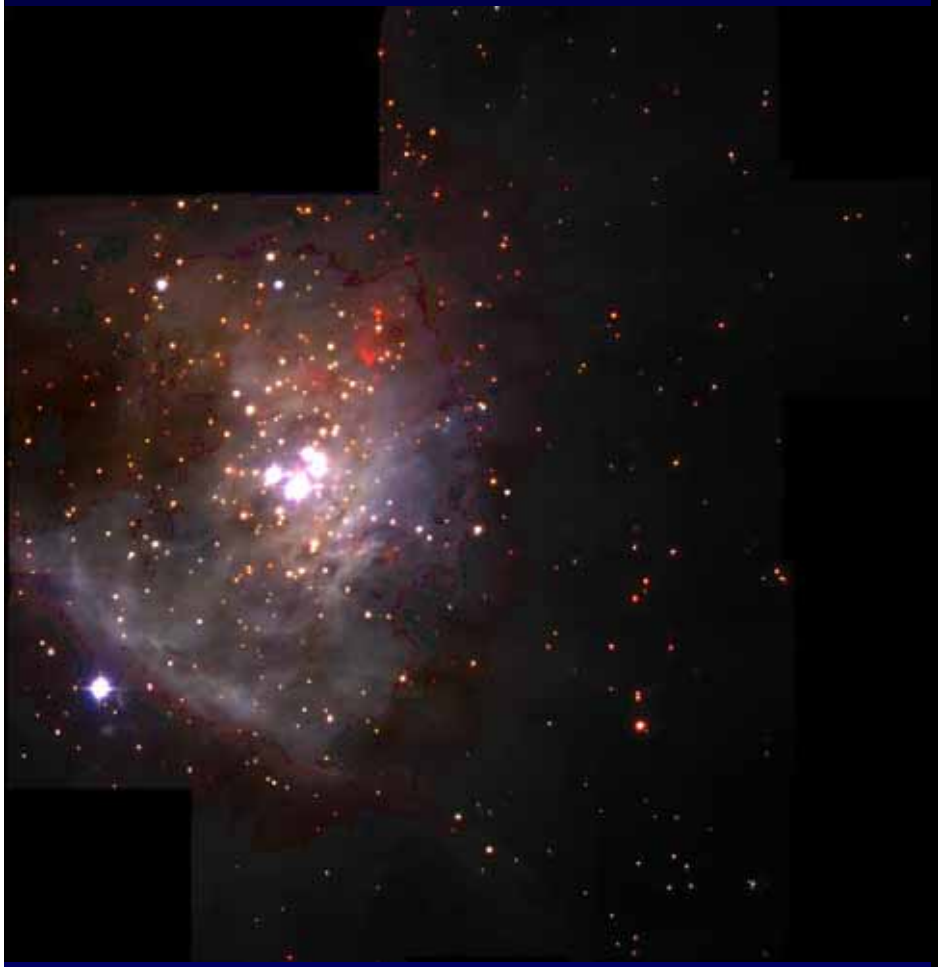

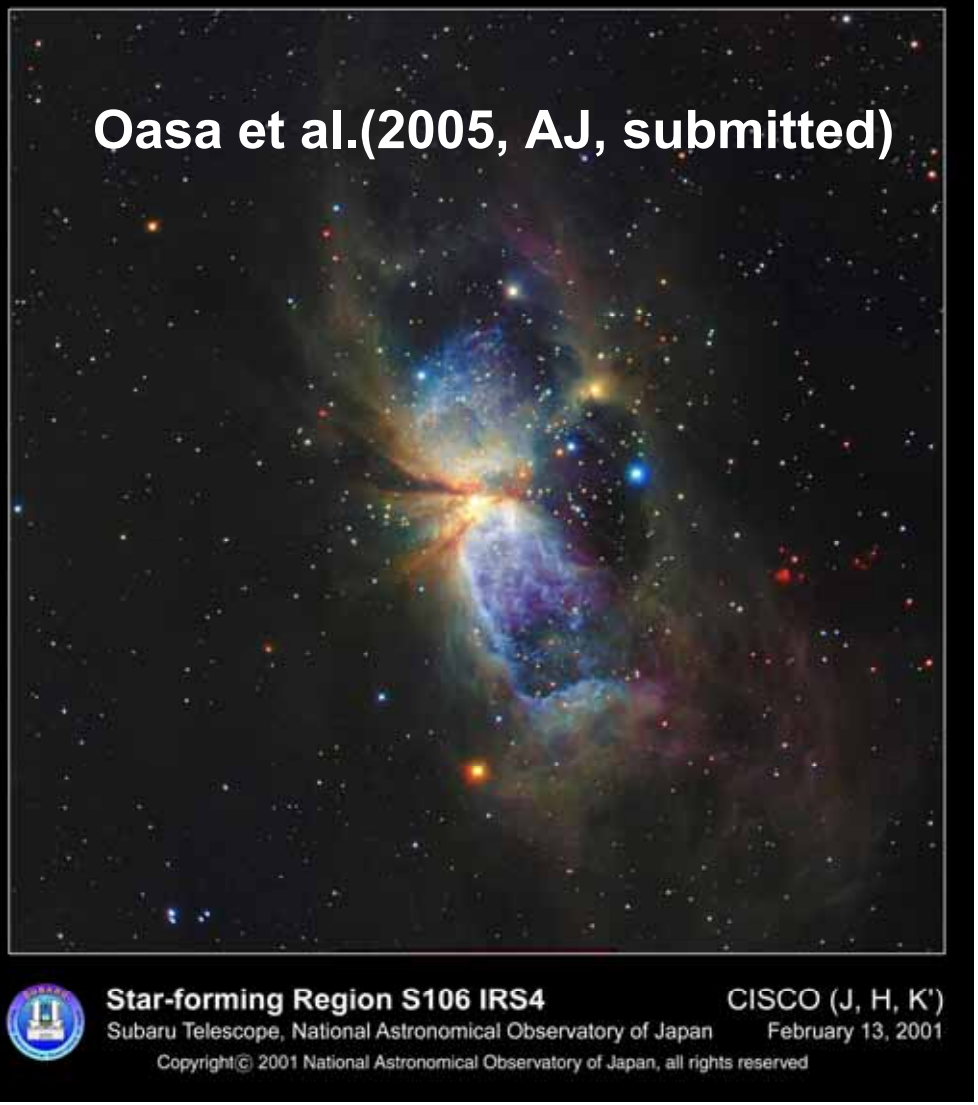

Planets in strange places

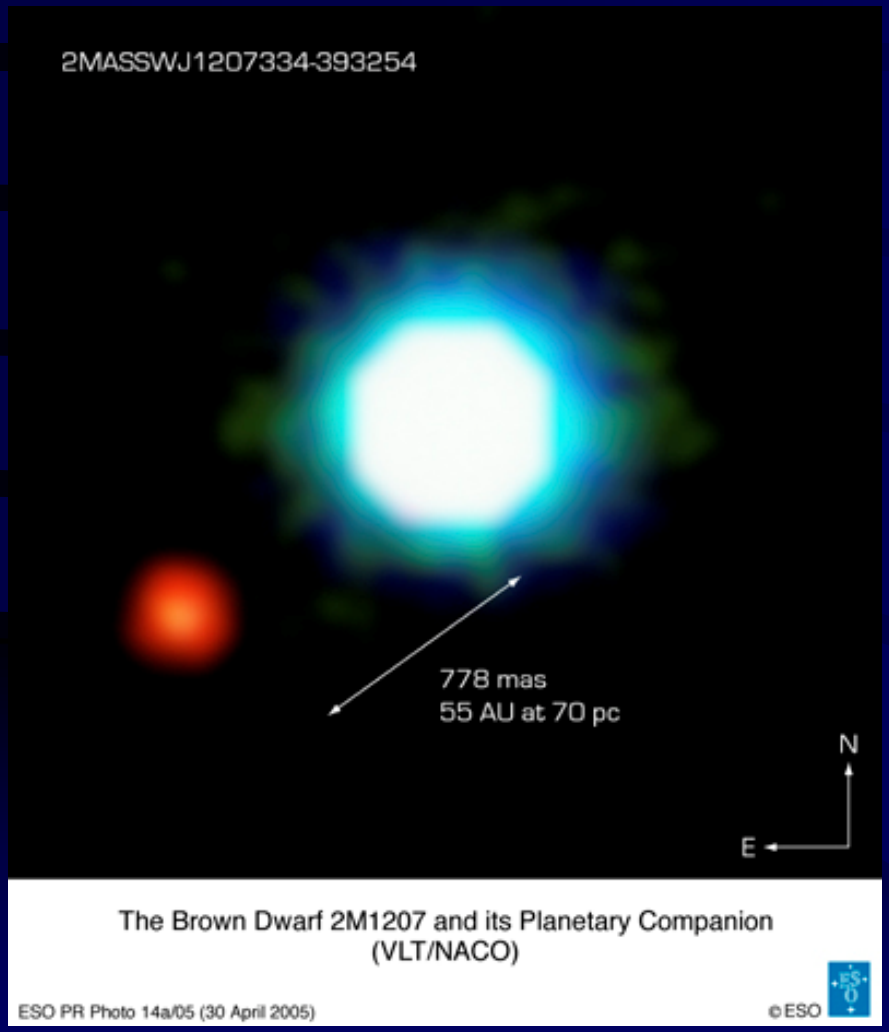

Recent discoveries

1) **2MASS 1207-3932,**

   A $5M_{Jup}$ planet orbiting a young (8Myr) brown dwarf at 55 AU separation.

   Chauvin et al.(2004; 2005)

2) **AB Pic,**

   A 13_{MJup} planet orbiting a young star at 275 AU. (Chauvin group).

3) **GQ Lup - a planet or brown dwarf orbiting a 1 Myr old star at 103 AU. Neuhauser et al. (2005)**

Spectroscopic follow up is in progress at Gemini, Subaru, VLT….

These NIRI spectra show clear confirmation of a ~13 Jupiter mass object as a Trapezium cluster member. Not enough sources have been observed yet to accurately quantify how many planetary mass objects there are.

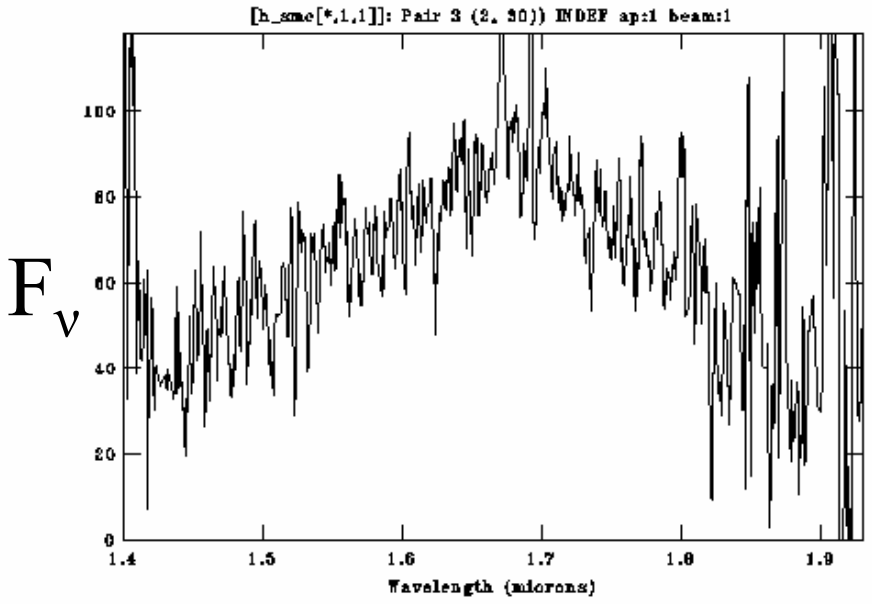

F_ν

H Band

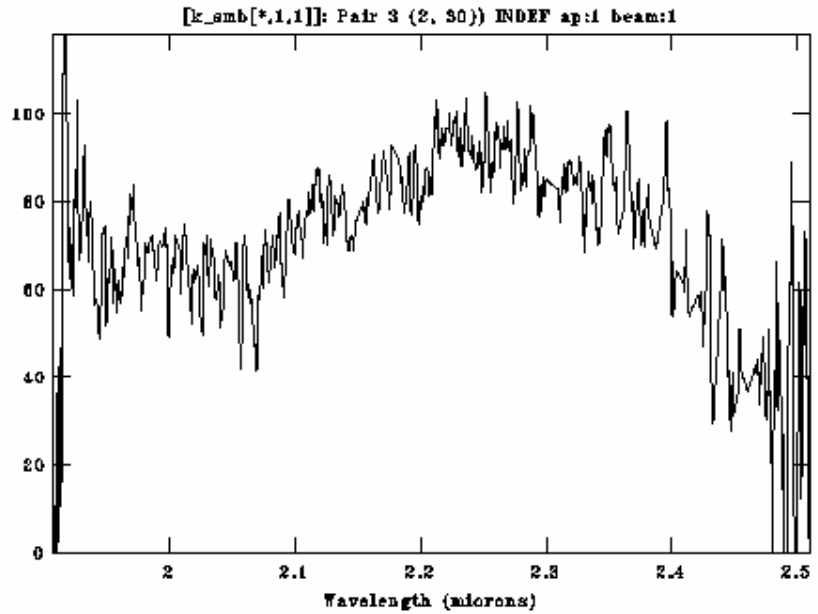

F_ν

K Band

Disks around Planetary Mass Objects?

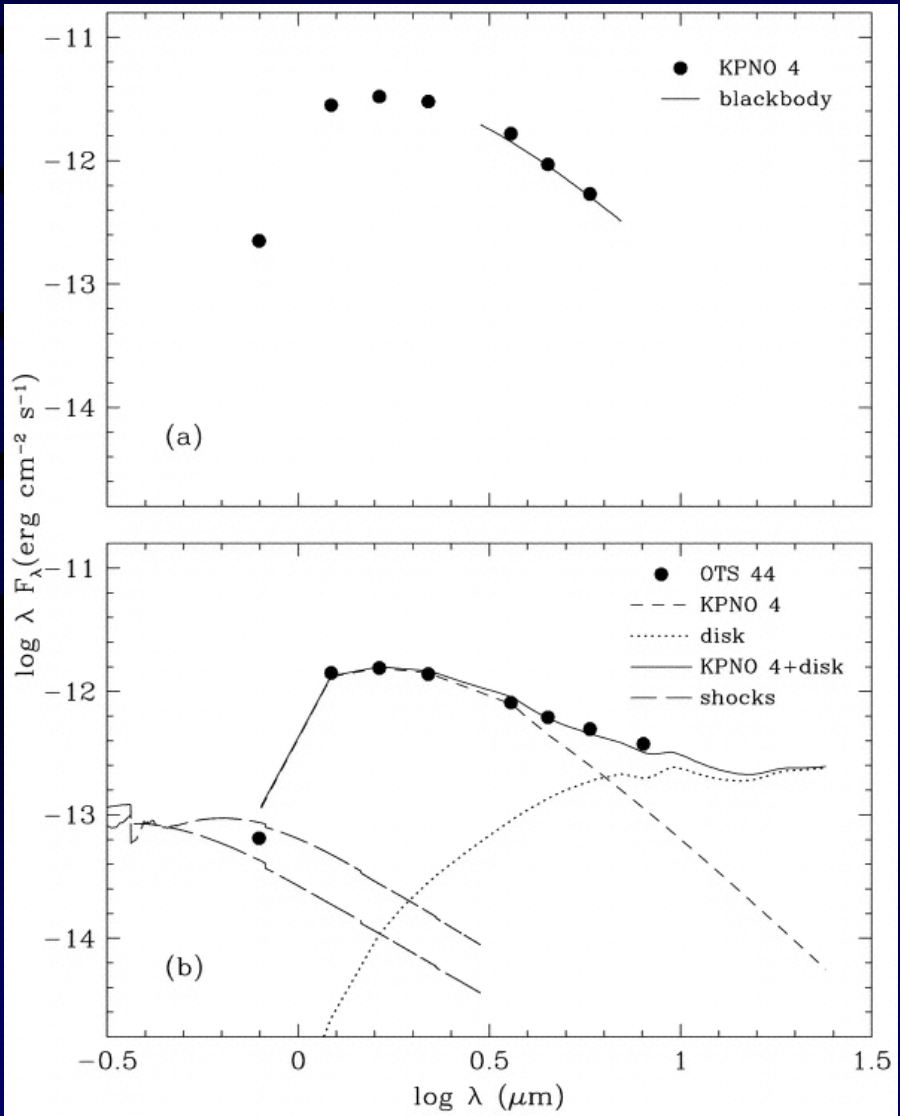

Recent observations with SPITZER (Luhman 2005) have found a large mid-IR excess around OTS44, an object in the Chameleon star formation region with M~15M_{Jup}.

Other very young brown dwarfs, eg. KPNO4 in Taurus, show no mid-IR excess.

Uncertainties in the masses

- The masses are not directly measured, merely deduced by comparison with theoretical model isochrones.
- The isochrones become unreliable below ages of a few Myr, since they do not take account of the star forming environment, e.g. accretion discs etc.
- Some recent observations suggest the deduced masses are quite accurate (Mohanty, Basri et al. 2004), while other works may indicate the masses are actually somewhat higher than we thought (Close et al.2005).
- These models are not appropriate for young planets formed by core accretion (Marley 2005). $E_{th} << GM^2/R$. This has consequences for all attempts to observe warm young planets (except externally heated hot Jupiters).

Burrows, Marley et al.1997

Uncertainties in the masses

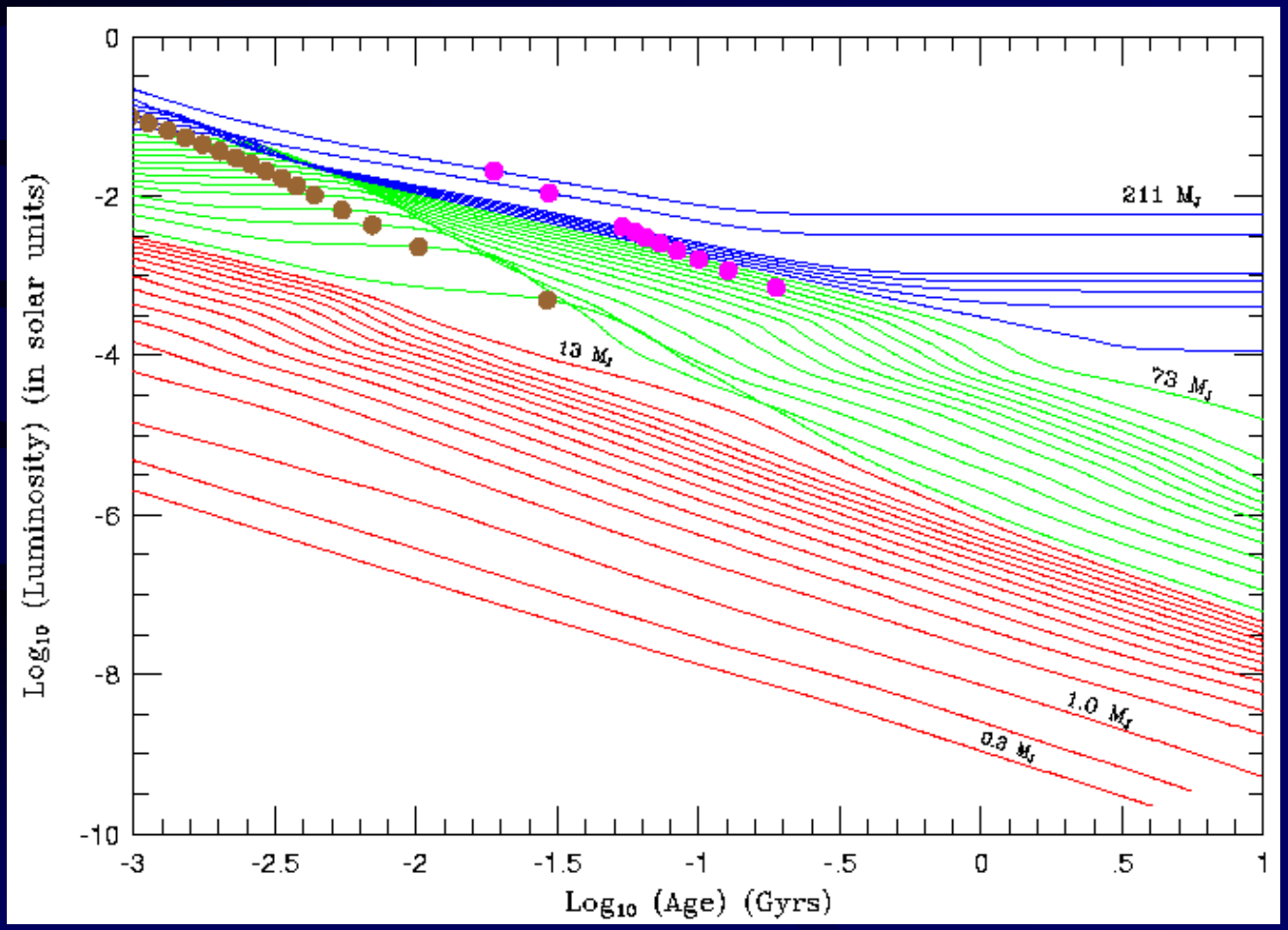

A confusing situation…

- **Masses of planets like 2M1207-3932b may be underestimated, but may be accurate if they formed like binary stars.**

- **How do we distinguish between different types of ‘cluster planet’:**

  (1) low mass brown dwarfs (which form like stars) or

  (2) core accretion planets which formed in wide orbits in a crowded star forming region and became unbound after an interaction with a passing star.

THE END